ACR No. L6B18

NATIONAL ADVISORY COMMITTEE FOR AERONAUTICS

WARTIME REPORT

ORIGINALLY ISSUED

March 1946 as
Advance Confidential Report L6B18

DEVELOPMENT OF WING INLETS

By Stanley F. Racisz

Langley Memorial Aeronautical Laboratory
Langley Field, Va.

WASHINGTON

NACA ACR No. L6B18

NATIONAL ADVISORY COMMITTEE FOR AERONAUTICS

ADVANCE CONFIDENTIAL REPORT

DEVELOPMENT OF WING INLETS

By Stanley F. Racisz

SUMMARY

An investigation was made in the Langley two-dimensional low-turbulence tunnels to develop a wing-inlet section having maximum lift and critical speeds as high as those of the corresponding basic airfoil section. Low inlet losses were desired for an extensive range of lift coefficient and flow rate. The investigation consisted in measurements of the lift, drag, internal-flow, and pressure-distribution characteristics of a low-drag-type airfoil section with several leading-edge air inlets. As a result of successive modifications, two wing-inlet sections having maximum lift coefficients exceeding the maximum lift coefficient of the basic airfoil section and negligible inlet losses throughout an extensive range of lift coefficient and inlet-velocity ratio have been developed. The critical Mach number of the inlet lips (the forward 0.50 chord) of one of the wing inlets was higher than that of the plain airfoil section. The critical Mach number of the entire wing-inlet section, however, was limited to a value somewhat lower than that of the plain airfoil section by the high suction pressures in the vicinity of the exit, which was located on the upper surface between 0.50 chord and 0.60 chord.

INTRODUCTION

Some of the more important problems involved in developing wing sections with leading-edge inlets for admitting cooling air are those of obtaining the required quantities of cooling air flow without excessive internal losses and of obtaining the desired maximum lift and critical speeds. Attempts to develop wing-inlet sections having the desired airfoil and cooling characteristics often result in some compromises.

A research program was undertaken in the Langley two-dimensional low-turbulence tunnels to develop a leading-edge air inlet for an airfoil section of the low-drag type. It was desired that the wing-inlet section have a maximum section lift coefficient of 1.26 at a Reynolds number of 3×10^6 and a critical Mach number of 0.67 at a section lift coefficient of 0.15, or values not lower than those for the plain airfoil section. The range of inlet-velocity ratio as a function of the lift coefficient for which low inlet losses were desired is shown in figure 1. Progressive modifications were made to a trial wing-inlet section of 2-foot chord in an attempt to develop a wing-inlet section having the desired characteristics. Although exact methods for determining wing-inlet profiles are not indicated by the data presented herein, an indication is given of the progress made in the development of a leading-edge air inlet for the airfoil section tested in this investigation.

The investigation consisted in measurements of the lift, drag, internal-flow, and pressure-distribution characteristics of several inlet configurations. Measurements of the characteristics were made through a range of angle of attack from negative lift coefficients to the stall. The investigation included tests of a wing inlet with roughness applied to the leading edges of the inlet lips to determine the effects of leading-edge roughness on the section characteristics.

SYMBOLS

The symbols and coefficients used in the presentation of results are as follows:

α_o section angle of attack, given with respect to reference line, degrees

c chord of original wing-inlet section measured along reference line

c_l section lift coefficient based on actual chord

c_d section drag coefficient based on actual chord

$c_{m_{c/4}}$ section pitching-moment coefficient at quarter-chord point

V velocity measured at point indicated by subscript

ρ mass density

μ coefficient of viscosity

q dynamic pressure $\left(\frac{1}{2}\rho V^2\right)$

H total pressure measured at point indicated by subscript

ΔH loss in total pressure measured at inlet or exit as indicated by subscript

h height between inlet walls measured at inlet or exit as indicated by subscript (fig. 2)

p local static pressure

δ_f wing flap deflection, degrees

R Reynolds number based on actual chord $\left(\frac{\rho_o V_o c}{\mu}\right)$

M_{cr} critical Mach number, that free-stream Mach number at which the speed of sound is first attained at any point on the airfoil surface

S pressure coefficient $\left(\frac{H_o - p}{q_o}\right)$

$\frac{V_i}{V_o}$ inlet-velocity ratio

Subscripts:

o free stream

i inlet

e exit

int internal

MODELS

The two-dimensional models tested in the investigation were constructed of laminated wood and had chords of 2 feet and spans of approximately 3 feet. Preparation of the surfaces for tests consisted in glazing local defects and then sanding the entire surfaces with No. 400 carborundum paper on rubber blocks.

The plain airfoil section, which formed the basic airfoil section for the wing-inlet sections, is similar to airfoils of the NACA 7-series (reference 1). At a section lift coefficient of 0.3, which is approximately the design lift coefficient, the chordwise positions of minimum pressure are approximately 0.35c and 0.50c for the upper and lower surfaces, respectively. The maximum thickness is approximately 0.17c. Two models, one with a plain trailing edge and one with a flap of 0.22c and a vane of 0.09c, were tested.

The external contours behind the 0.19¼c station of the wing-inlet section were the same as those of the plain airfoil section. The trial inlet, designated herein the original inlet (fig. 2), had small leading-edge radii and lip stagger, and represented a configuration which might be expected to minimize the length of fairing that would be required between the plain airfoil and the ducted sections of a full-scale wing. The cooling air exhausted over the upper surface slightly downstream of the 0.50c position, and the air flow was regulated by an internal exit flap pivoting at the 0.60c station. Such an exit configuration is one that might be designed for a flapped airfoil section. The inlet and exit of the ducted model extended across the entire span.

TEST METHODS

Test data at a Reynolds number of approximately 2.5×10^6 were obtained in the Langley two-dimensional low-turbulence tunnel (designated LTT). Test data at Reynolds numbers of approximately 6×10^6 and 9×10^6 were obtained in the Langley two-dimensional low-turbulence pressure tunnel (designated TDT). Lift data were obtained from pressure measurements along the floor and ceiling of the tunnel test section. Drag

characteristics were determined from wake-survey measurements. Details of the test methods for the two-dimensional low-turbulence tunnels are discussed in reference 1.

Surface pressures for the wing-inlet section were measured with small static tubes of 0.040-inch outside diameter which were mounted close to the airfoil surface. Orifices in the model surfaces were used to measure the pressure-distribution characteristics of the plain airfoil section.

Flow measurements were made at both the inlet and exit of the ducted section to determine the inlet loss, the inlet-velocity ratio, and the total-pressure loss through the ducted section. The inlet loss was determined from measurements made with three total-pressure tubes located at the 0.10c station as shown in figure 2. The inlet-velocity ratio and the loss in total pressure were determined from measurements of flow at the exit. Measurements of the flow at the exit were made with a rake consisting of one static-pressure and four total-pressure tubes having outside diameters of approximately 0.040 inch. Small exit heights permitted the use of only two or three total-pressure tubes. For large exit heights, two or more survey rakes located at several spanwise stations were used to determine the average exit flow.

The internal drag coefficient was determined from the following equation, which neglects changes in density:

$$c_{d_{int}} = \frac{2h_e V_e}{cV_o}\left(1 - \sqrt{1 - \frac{\Delta H_e}{q_o}}\right)$$

No heat was added to simulate actual cooling conditions.

The test data have been corrected for tunnel-wall effects, according to the methods discussed in reference 1, by the following equations:

$$c_l = 0.987c_l'$$

$$c_d = 0.988c_d'$$

$$c_{mc/4} = 0.990c_{mc/4}'$$

$$a_o = 1.015a_o'$$

$$q_o = 1.012q_o'$$

where the primed quantities represent the values measured in the tunnel. All test data were obtained at free-stream Mach numbers less than 0.17.

RESULTS AND DISCUSSION

Plain Airfoil Section

The lift, drag, and pitching-moment characteristics of the plain airfoil section at Reynolds numbers of 3×10^6, 6×10^6, and 9×10^6 and the characteristics of the airfoil section with a double-slotted flap are presented in figure 3(a). The effects of the double-slotted flap on the lift and pitching-moment characteristics are of the order expected for this type of high-lift device. The increase in the minimum section drag coefficient caused by standard leading-edge roughness (reference 1) is similar to that obtained for other airfoil sections of this type. The pressure-distribution characteristics of the plain airfoil section are presented in figure 3(b). These data indicate that the range of section lift coefficient giving a favorable pressure gradient over the forward portion of the airfoil extends from a section lift coefficient of -0.04 to slightly less than 0.50. The peak pressure coefficient at a section lift coefficient of 0.15 corresponds to a critical Mach number (estimated by the methods of reference 2) of 0.67.

Original Wing-Inlet Configuration

Figure 4 presents the characteristics of the wing-inlet section with the original inlet. A comparison of the lift characteristics, presented in figure 4(a), with those of the plain airfoil section (fig. 3(a)) indicates a 22-percent reduction in the maximum section lift coefficient. Test data at Reynolds numbers up to 6×10^6 (not presented) indicated no favorable scale effects on the maximum section lift coefficients.

Initial tests of the model were made with no internal resistance. The data presented in figure 4(b) show that the inlet loss is low for only a small range of lift coefficient. The rapid rise in the inlet losses causes high total-pressure losses through the ducted section, as indicated by the total-pressure loss measured at the exit (fig. 4(a)). The high internal losses probably cause excessively thick boundary layers behind the exit and consequently the high drag shown in figure 4(a). The pressure-distribution data presented in figures 4(c) and 4(d) indicate the critical Mach number for the first 0.50c to be 0.66 at a section lift coefficient of 0.22 and an inlet-velocity ratio of 0.28. The critical Mach number of the entire wing-inlet section, however, is reduced to 0.63 because of the peak pressure in the vicinity of the exit. Under all conditions tested, the critical Mach number was limited by the high suction pressures in the vicinity of the exit.

Inlet 2

In an attempt to increase the maximum section lift coefficient, the leading-edge radii of the inlet lips were increased. The lip stagger was increased to permit the upper lip to guide the air flow into the inlet at high angles of attack, and the inlet-velocity ratio for a given exit opening was reduced by increasing the inlet height. These modifications, which were made in an attempt to reduce the inlet loss at high lift coefficients, are shown in figure 5.

The section characteristics of the ducted model with inlet 2 are presented in figure 6. A comparison of the lift characteristics with those of the original inlet (fig. 4(a)) indicates that the maximum section lift coefficient was considerably increased and exceeded that of the plain airfoil section (fig. 3(a)). The increase in the maximum section lift coefficient can be attributed largely to the increased lip radii. The drag characteristics, presented in figure 6(a), indicate that the rapid rise in the section drag coefficient occurs at higher lift coefficients in comparison to that obtained for the original inlet (fig. 4(a)). At high lift coefficients, the inlet losses of inlet 2 are lower than those of the original inlet; and the range of lift coefficient for low inlet loss is therefore more extensive (figs. 4(b) and 6(b)). The inlet losses at low

lift coefficients, however, are somewhat excessive. Several modifications were made in attempts to obtain low inlet losses at low lift coefficients without increasing the inlet losses at high lift coefficients. Successive attempts led to the development of inlet 3.

Inlets 3 and 4

Inlet 3.- Preliminary tests of the trial inlet shapes, which led to the development of inlet 3, indicated that the range of lift coefficient for low inlet loss can be shifted slightly by varying the inlet lip stagger. The lip stagger was therefore decreased, as shown in figure 7, in an attempt to decrease the inlet losses at low lift coefficients. In an effort to compensate for the expected increase in the inlet loss at high lift coefficients, the lips were thickened internally to form a gradually expanding diffuser that would tend to allow the upper lip to guide the internal flow. In like manner, at low lift coefficients the lower lip would tend to guide the internal flow.

Figure 8 shows the exit modifications that were made to increase the exit area. The exit modifications consisted in increasing the camber and chord of the exit flap and, because of the larger flap chord, it was necessary to modify the exit lip as shown in the sketch. Previous configurations of the ducted airfoil section were tested without simulated heat-exchanger resistance. The ducted section with inlet 3 was tested with a baffle plate simulating heat-exchanger resistance in order to include the effects of internal resistance on the section characteristics. The position of the simulated heat-exchanger in the inlet and its construction are shown in figures 7 and 9, respectively. The baffle plate had a ratio of open area to total area of 0.67.

Figure 10 presents the section characteristics of the wing-inlet section with inlet 3. A comparison of the lift characteristics presented in figure 10(a) with those of the plain airfoil section (fig. 3(a)) shows that the maximum section lift coefficient is considerably higher than that of the plain airfoil section. Figure 10(a) also shows that the inlet losses are negligible for an extensive range of inlet-velocity ratio and lift coefficient. The low inlet losses can be attributed

to the fact that separation at the inlet is probably prevented by the guiding action of the inlet lips. Figure 10(b) shows the pressure distributions over the lower lip. The critical Mach number corresponding to the peak pressure coefficient at a section lift coefficient of 0.13 is 0.51, or considerably lower than that of the plain airfoil section. Attempts were therefore made to increase the critical Mach number by thickening the external lower lip with modeling clay to form inlet 4.

Inlet 4.- Figure 7 shows the modifications made to form inlet 4. A comparison of the pressure distributions over the lower lip of inlet 4 (fig. 11) with those obtained over the lower lip of inlet 3 (fig. 10(b)) indicates the critical speed of inlet 4 to be higher than that of inlet 3. The critical Mach number of the lower lip of inlet 4 is 0.68 at a section lift coefficient of 0.28, or slightly higher than that of the plain airfoil section. The slightly lower maximum section lift coefficient of inlet 4 (fig. 11). may have been caused by a change in the inlet-velocity ratio or by some surface irregularities inasmuch as the lower lip of inlet 4 was constructed of modeling clay. The internal-flow characteristics of inlet 4 should be similar to those of inlet 3 because the inlets have the same profiles with the exception of the external lower lip. The section characteristics of inlet 4 are therefore more favorable than those of inlet 3 because of the higher critical Mach number of the lower lip.

Although the section characteristics of inlet 4 may be considered satisfactory, this inlet has the structural disadvantage of requiring an extensive fairing between the ducted and plain airfoil sections. An attempt was consequently made to develop an inlet configuration that could be faired into the plain airfoil section without an extensive blister.

Inlet 5

Smooth model.- Figure 12 is a sketch of inlet 5, which was developed from tests of a trial configuration. The internal contours were similar to those of inlet 3, but the leading edge of the inlet was located farther rearward to retain approximately the same inlet height as that of inlets 3 and 4 without extending the external contours beyond those of the plain airfoil section.

Figures 13(a) to 13(e) present the characteristics of the ducted section in the smooth condition. A comparison of these lift characteristics (fig. 13(a)) with those of the plain airfoil section (fig. 3(a)) indicates that the maximum section lift coefficient of the ducted section is at least as high as that of the plain airfoil section for an extensive range of inlet-velocity ratio. The data presented in figure 13(b) indicate negligible inlet losses for the desired range of lift coefficient and inlet-velocity ratio shown in figure 1. The pressure distributions shown in figures 13(c) and 13(d) indicate an extensive range of lift coefficient for a favorable pressure gradient over the upper and lower inlet lips.

The critical Mach number of the inlet lips (the forward 0.50c) is 0.67 at a section lift coefficient of 0.15 and at an inlet-velocity ratio of 0.3, or slightly higher than that of the plain airfoil section. The high suction pressures in the vicinity of the exit, however, reduce the critical Mach number of the entire wing-inlet section to 0.61. An increase in the critical Mach number of the ducted wing section can probably be obtained by locating the exit farther rearward or by undercutting the exit (as shown in reference 3) and extending the exit lip to direct the exit flow parallel to the airfoil surface.

Lift, drag, and flow data at a Reynolds number of 6×10^6 are presented in figure 13(e). A comparison of the lift characteristics with those obtained at a Reynolds number of 2.3×10^6 (fig. 13(a)) indicates favorable scale effects on the maximum section lift coefficient. The minimum section drag coefficient (fig. 13(e)) is considerably higher than that expected for a plain airfoil section having pressure-distribution characteristics similar to those of inlet 5. The increase in the minimum section drag coefficient may therefore be attributed largely to the exit flow.

Leading-edge roughness.- Test data showing the effects of leading-edge roughness on the lift and flow characteristics are presented in figure 13(f). These data indicate that leading-edge roughness on one or both inlet lips causes no appreciable change in the internal-

flow characteristics. The maximum section lift coefficient is unaffected by leading-edge roughness on the lower inlet lip. A comparison of the lift characteristics for both the smooth and rough conditions indicates that leading-edge roughness on the upper inlet lip reduces the maximum section lift coefficient by approximately the same decrement as that obtained for the plain airfoil section (fig. 3(a)).

Transition Section

The fairing required between the plain airfoil section and inlet 5 is somewhat large, and a substantial decrease in the maximum section lift coefficient might be obtained on a three-dimensional wing because of the shape of the inlet end closure. Tests were therefore made of a half-span ducted airfoil section with inlet 5 to give an indication of the effects of the leading-edge fairing on the lift characteristics. The transition section was formed by attaching the leading-edge contour of the plain airfoil section to the wing-inlet section with inlet 5 to form a half-span ducted airfoil section. Figure 14 shows various views of the model and the fairing between the plain and ducted airfoil sections. A partition between the ducted and plain airfoil sections restricted the internal flow to the ducted airfoil section.

A comparison of the lift characteristics presented in figure 15 with those of the plain airfoil section (fig. 3(a)) indicates that the maximum section lift coefficient of the transition section is nearly the same as that of the plain airfoil section. The drag data presented in figure 15 indicate that stalling first occurs over the plain airfoil section.

Comparison of Characteristics of Ducted and Plain Airfoil Sections

Maximum lift.- The variation of maximum section lift coefficient with inlet-velocity ratio is shown in figure 16(a). The highest maximum section lift coefficients were obtained with inlet 4. The maximum section lift coefficient of the ducted model with inlet 4 is higher than that of the plain airfoil section for

inlet-velocity ratios ranging from a value somewhat less than 0.30 up to a value of 1.26. The maximum section lift coefficient of the ducted airfoil section with inlet 5 is higher than that of the plain airfoil section for inlet-velocity ratios between 0.13 and 0.85.

Inlet losses.- Figure 16(b) shows the range of lift coefficient and inlet-velocity ratio at which the inlet loss is negligible. Inlet 4 has negligible inlet losses for a more extensive range of inlet-velocity ratio and lift coefficient as compared with those of inlets 1 and 5. Negligible inlet losses throughout the range of inlet-velocity ratio and lift coefficient at which low inlet losses are generally desired can be obtained with either inlet 4 or inlet 5.

Critical Mach number.- Figure 16(c) shows the critical Mach number of inlet 5 (the forward 0.50c) and the critical Mach number of the plain airfoil section. At the high-speed condition, the critical Mach number is slightly higher than that of the plain airfoil section.

Effect of exit on critical Mach number.- Figure 16(d) shows the critical Mach number corresponding to the peak pressure over the exit flap for both the original and modified exits. A comparison of figures 16(d) and 16(c) indicates that the peak pressure over the exit flap reduces the critical Mach number by approximately 0.06 at the high-speed condition. These data indicate that an important factor to be considered in the design of an exit is the effect of the exit on the critical Mach number.

CONCLUSIONS

As the result of an investigation of a low-drag airfoil section with several leading-edge air inlets in the Langley two-dimensional low-turbulence tunnels, two leading-edge air inlets having the following characteristics have been developed:

(1) Maximum lift coefficients higher than the maximum lift coefficient of the plain airfoil section for an extensive range of inlet-velocity ratio

(2) Negligible inlet losses for an extensive range of inlet-velocity ratio and lift coefficient

The critical Mach number of one of the wing inlets (the forward 0.50c) was slightly higher than that of the plain airfoil section. The critical Mach number of the entire wing-inlet section, however, was limited to a value somewhat lower than that of the plain airfoil section by the high suction pressures in the vicinity of the exit which was located on the upper surface between 0.50 chord and 0.60 chord.

Langley Memorial Aeronautical Laboratory
National Advisory Committee for Aeronautics
Langley Field, Va.

REFERENCES

1. Abbott, Ira H., von Doenhoff, Albert E., and Stivers, Louis S., Jr.: Summary of Airfoil Data. NACA ACR No. L5C05, 1945.

2. von Kármán, Th.: Compressibility Effects in Aerodynamics. Jour. Aero. Sci., vol. 8, no. 9, July 1941, pp. 337-356.

3. Becker, John V., and Baals, Donald D.: High-Speed Tests of a Ducted Body with Various Air-Outlet Openings. NACA ACR, May 1942.

L-727

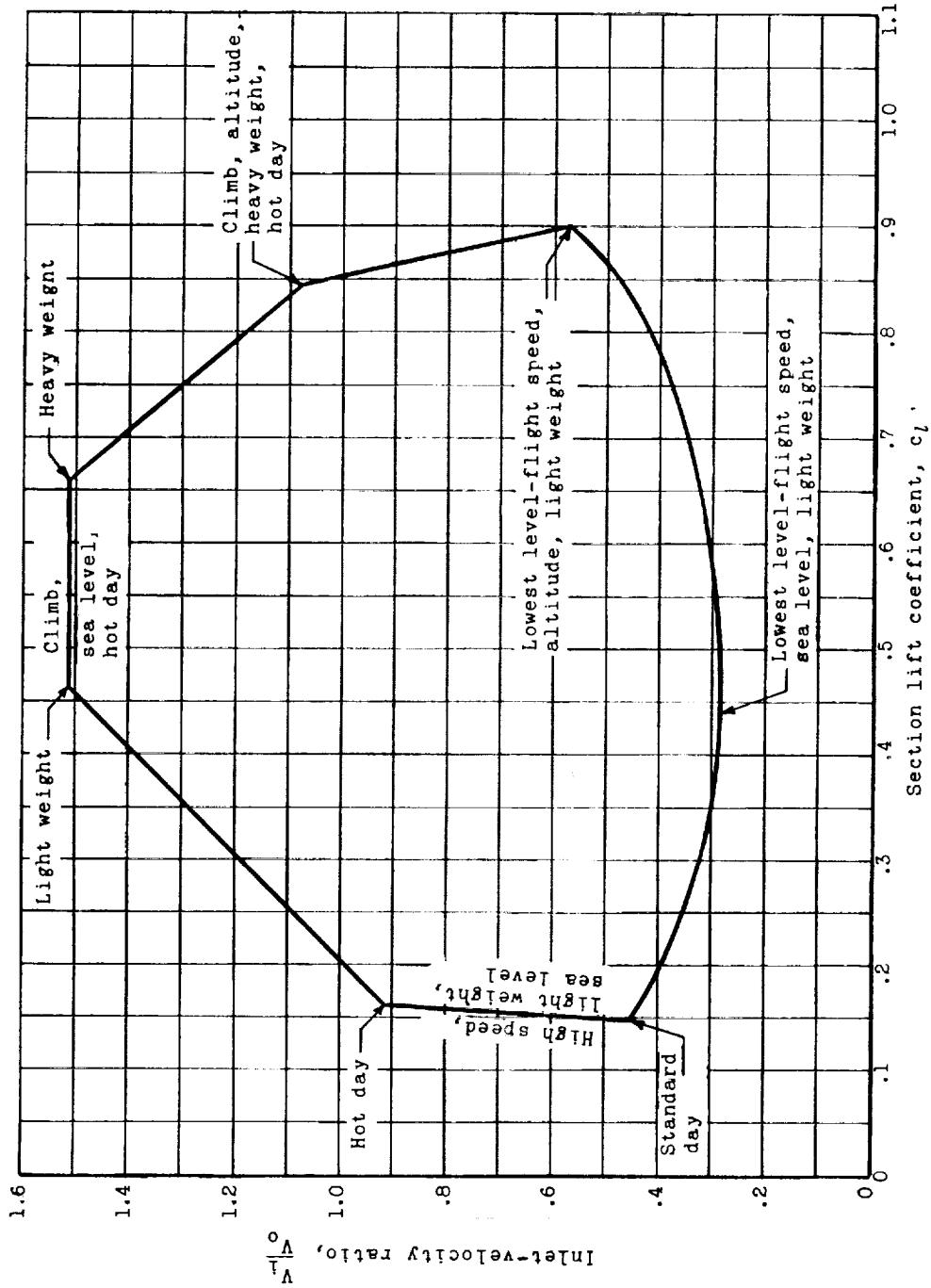

Figure 1.- Variation of inlet-velocity ratio with lift coefficient for various flight conditions.

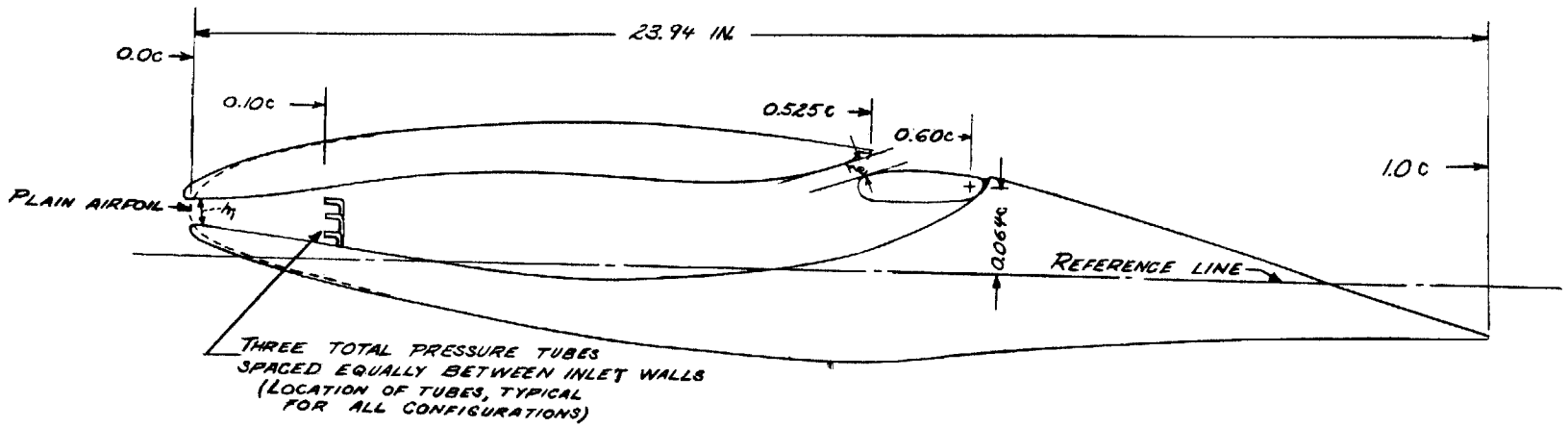

Figure 2.- Profile of original configuration of wing inlet section.

L-727

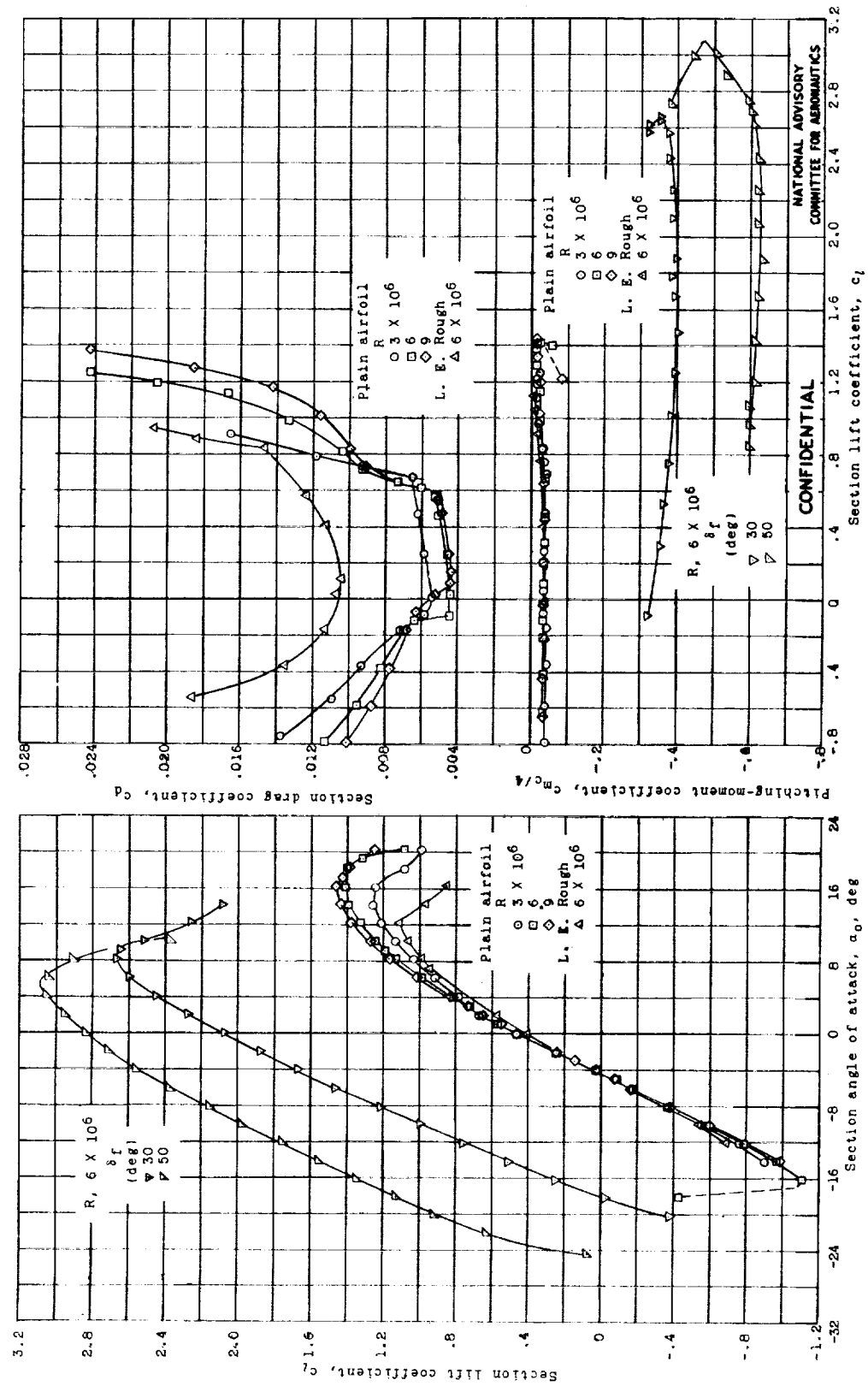

(a) Lift, drag, and pitching-moment characteristics.

Figure 3.- Aerodynamic characteristics of the plain airfoil section: tests, TDT 524-5, 586, and 769.

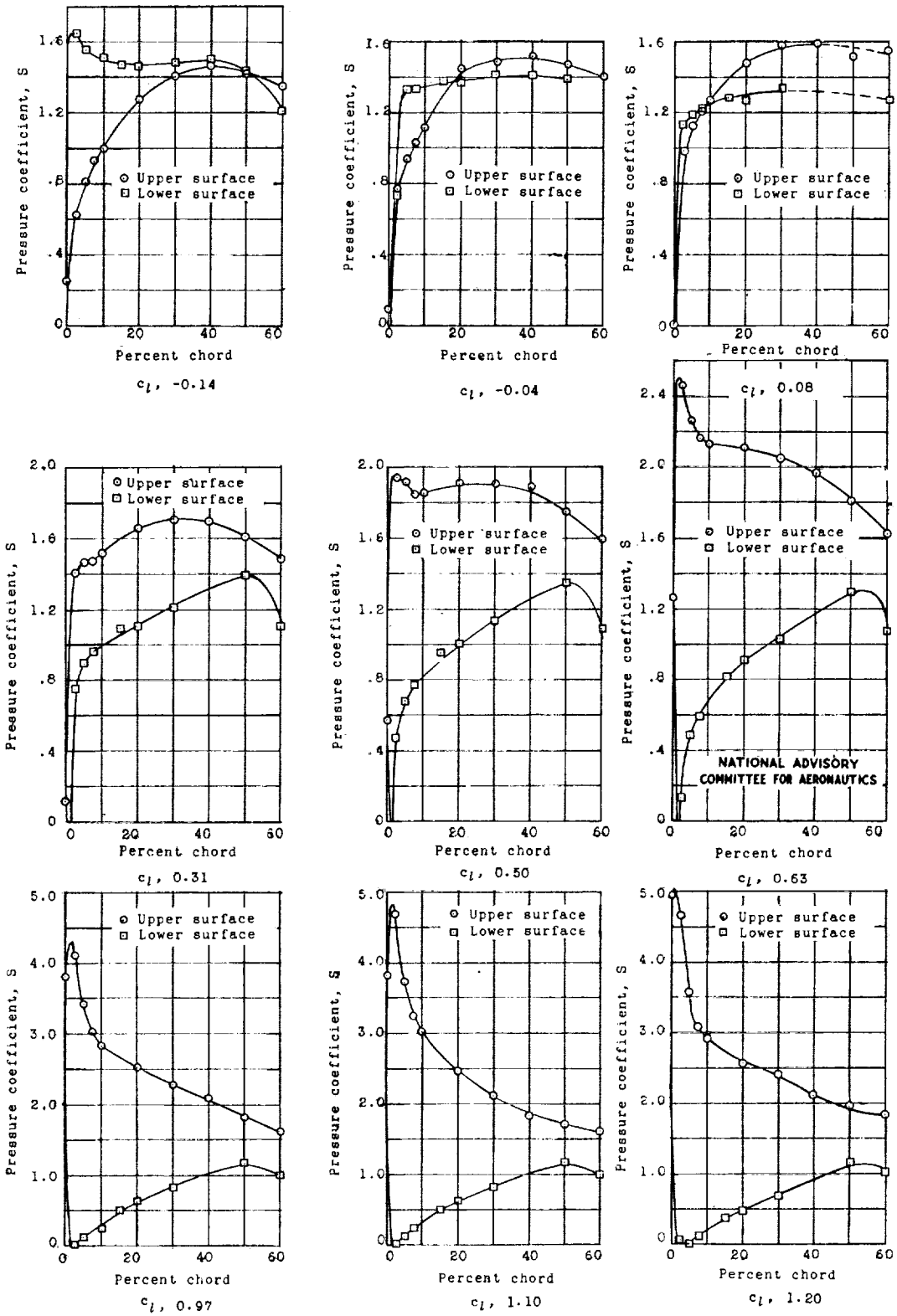

(b) Pressure distributions for plain airfoil; R, 6 X 10^6.

Figure 3 .- Concluded.

L-727

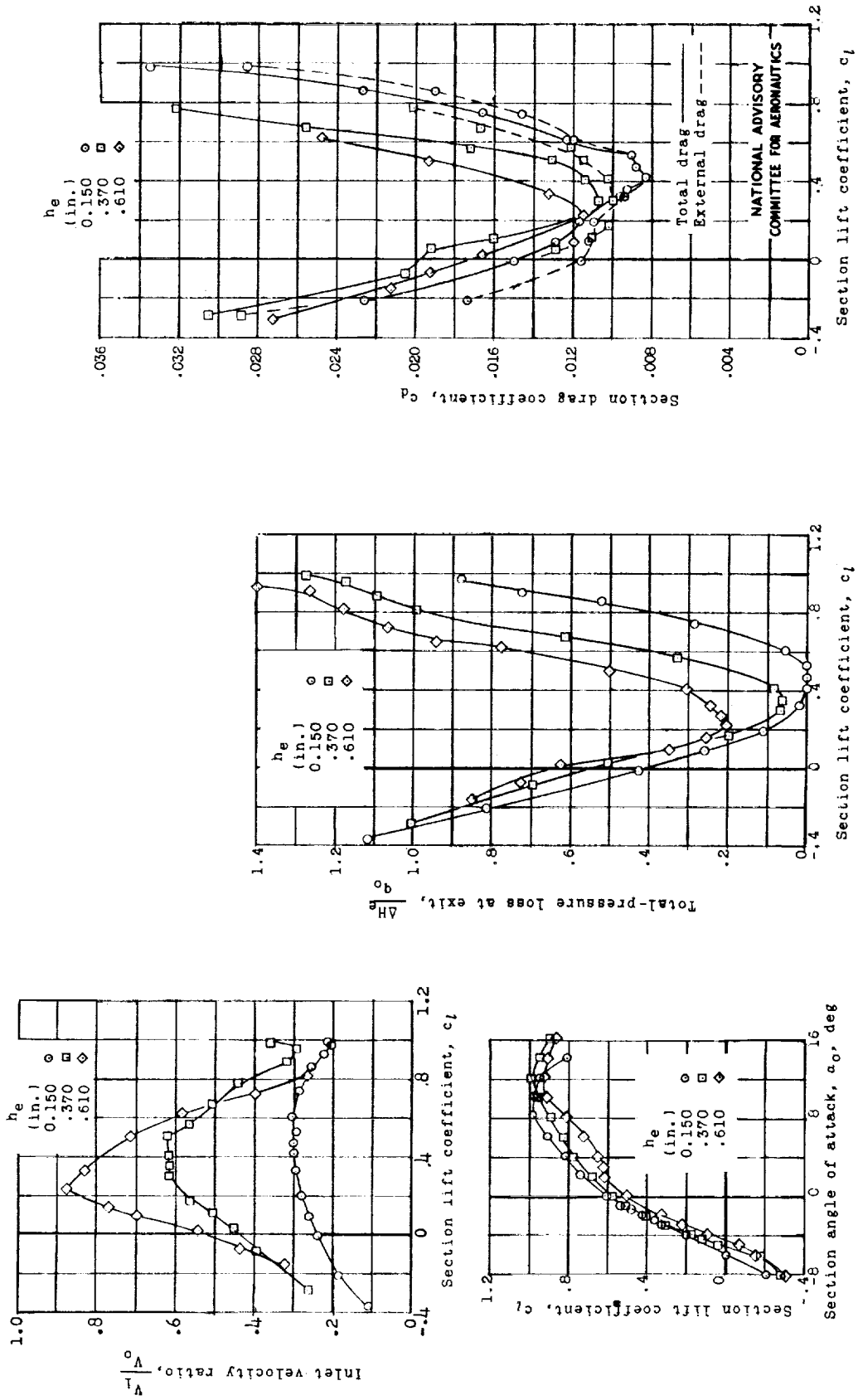

(a) Lift, drag, and flow characteristics; R, 3 X 10^6.

Figure 4.- Aerodynamic characteristics of the original configuration of the wing-inlet section; tests, TDT 679 and LTT 353.

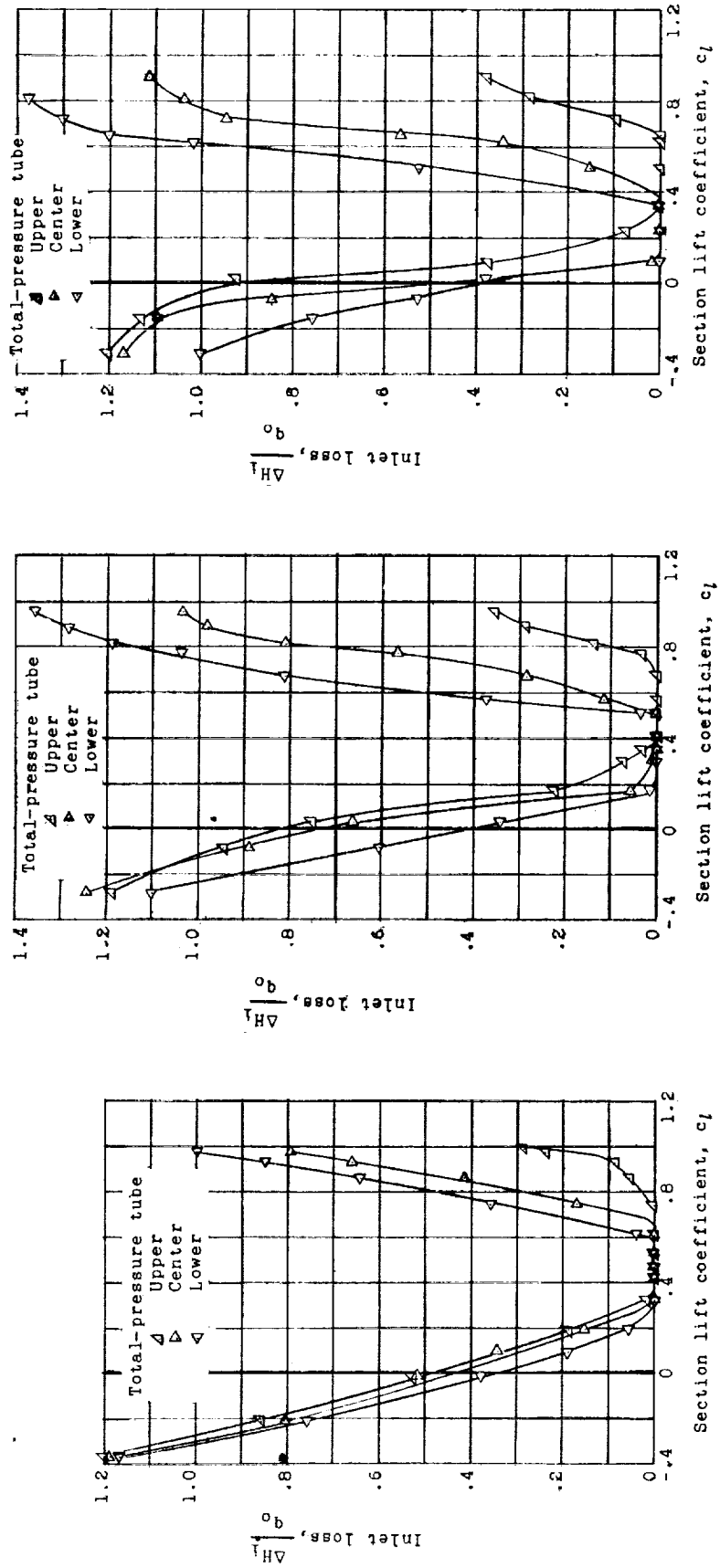

NATIONAL ADVISORY COMMITTEE FOR AERONAUTICS

(b) Inlet losses; R, 3 X 10^6.

Figure 4 - Continued.

L-727

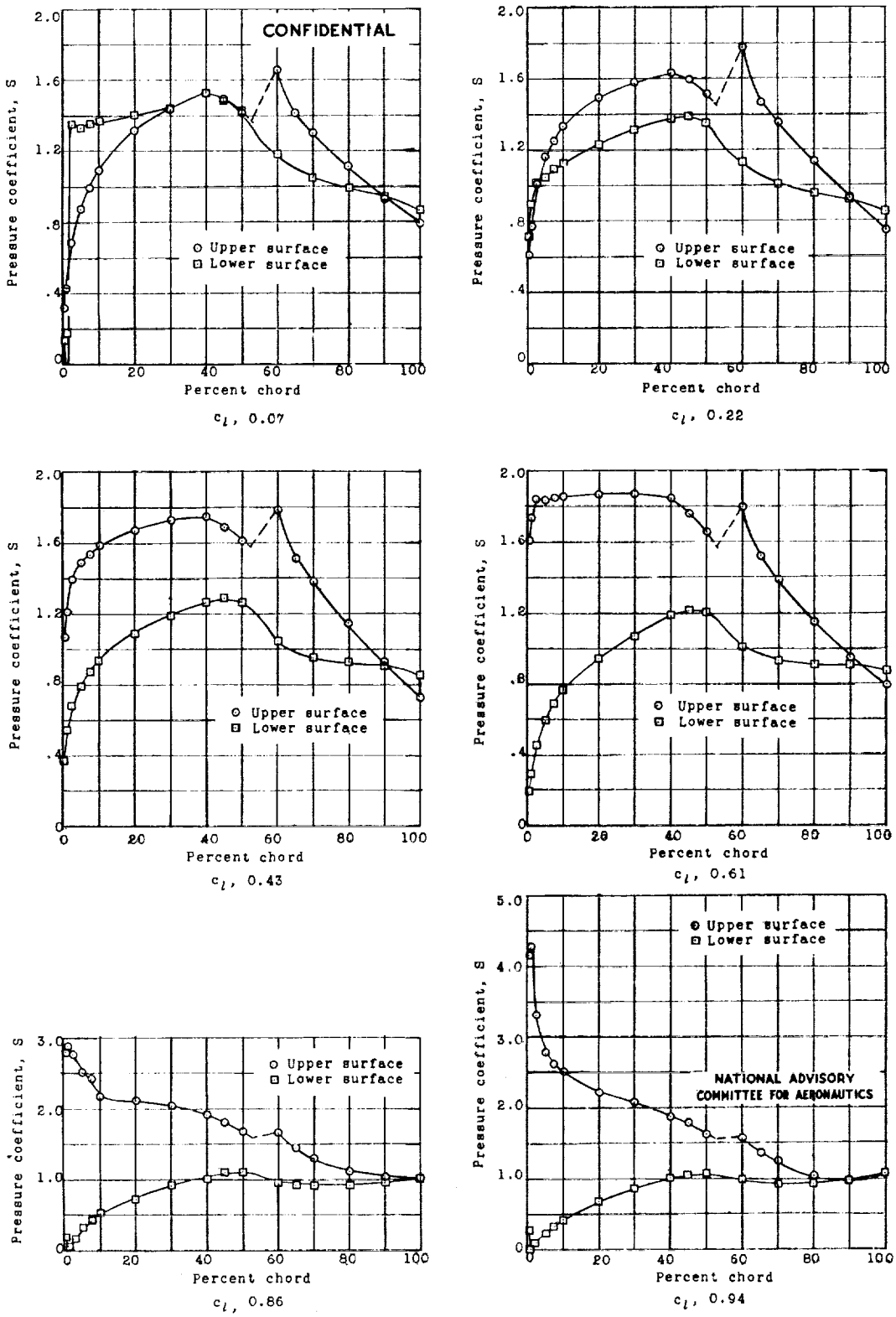

(c) Pressure distributions; h_e, 0.150 inches; R, 2.4 X 10^6.

Figure 4.- Continued.

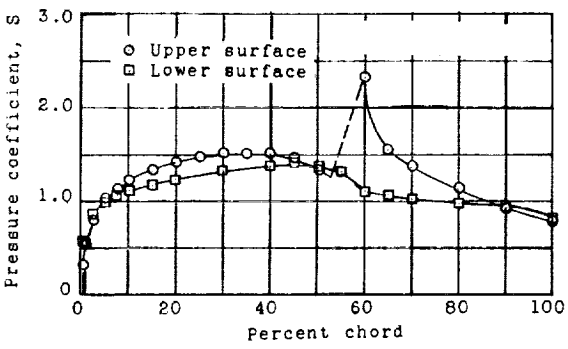

c_l, 0.16

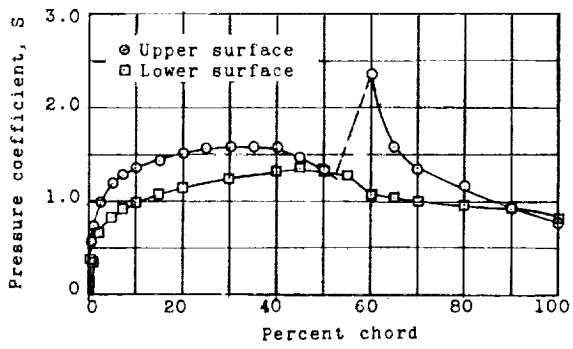

c_l, 0.28

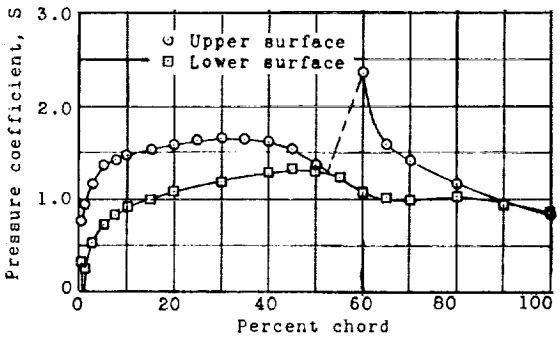

c_l, 0.38

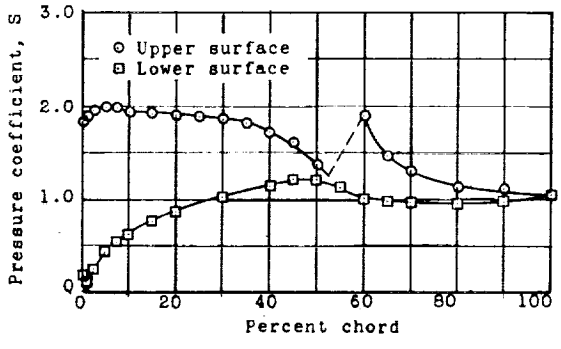

c_l, 0.62

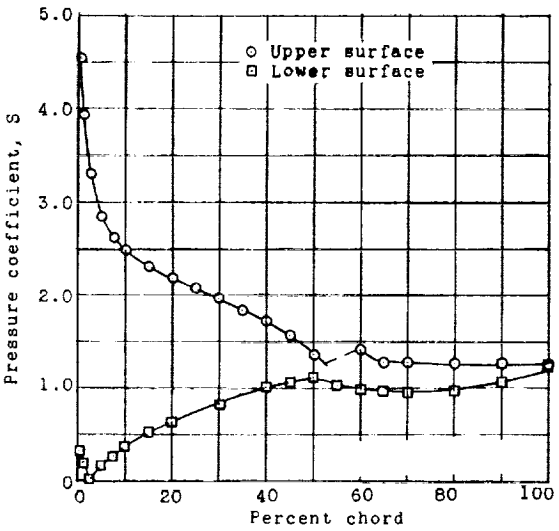

c_l, 0.86

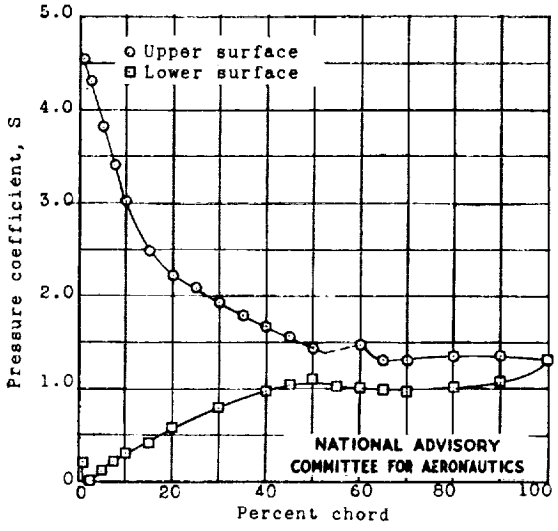

c_l, 0.93

(d) Pressure distributions; h_e, 0.610 inches; R, 2.4 X 10^6.

Figure 4.- Concluded.

L-727

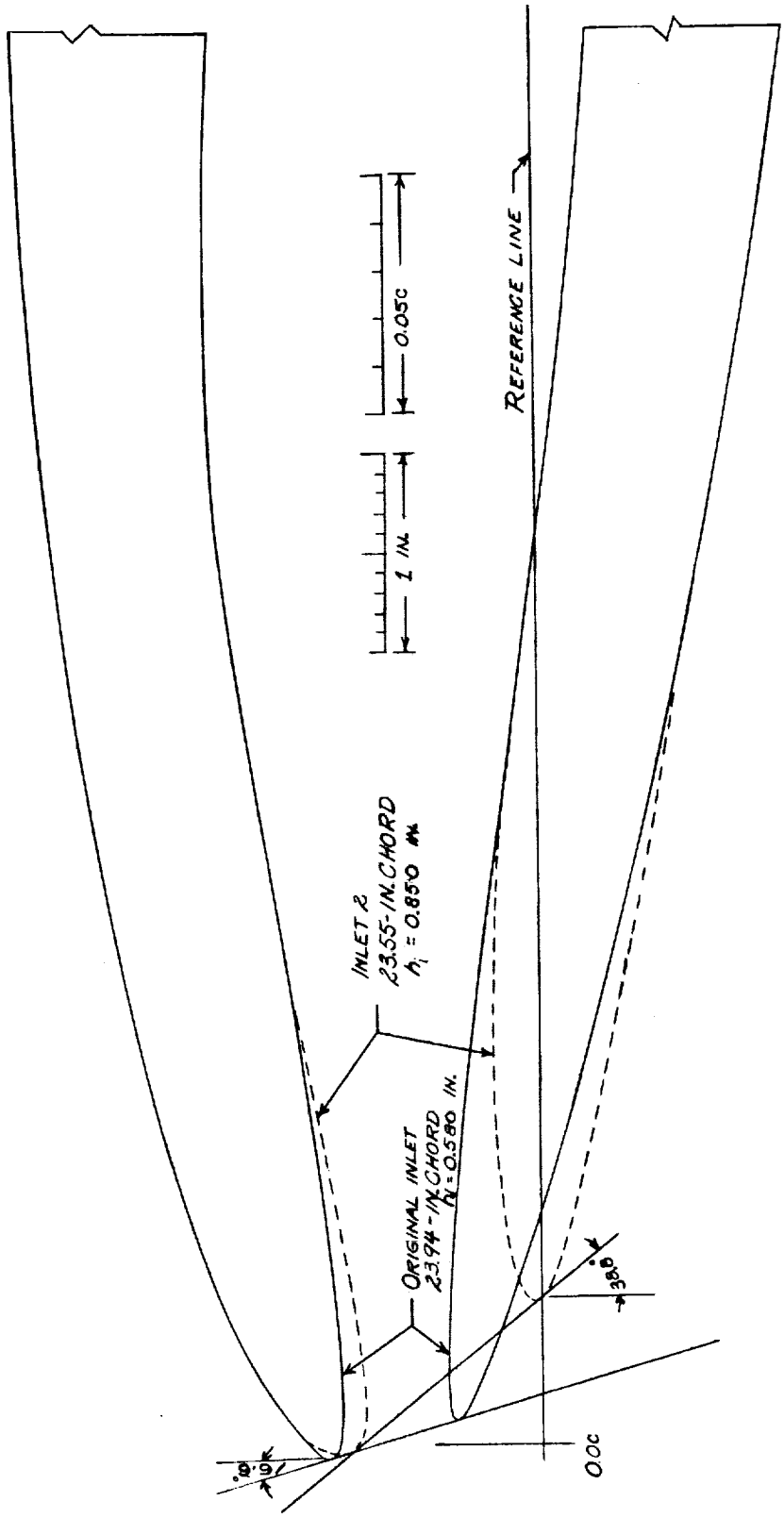

Figure 5.- Profiles of the original and modified inlets.

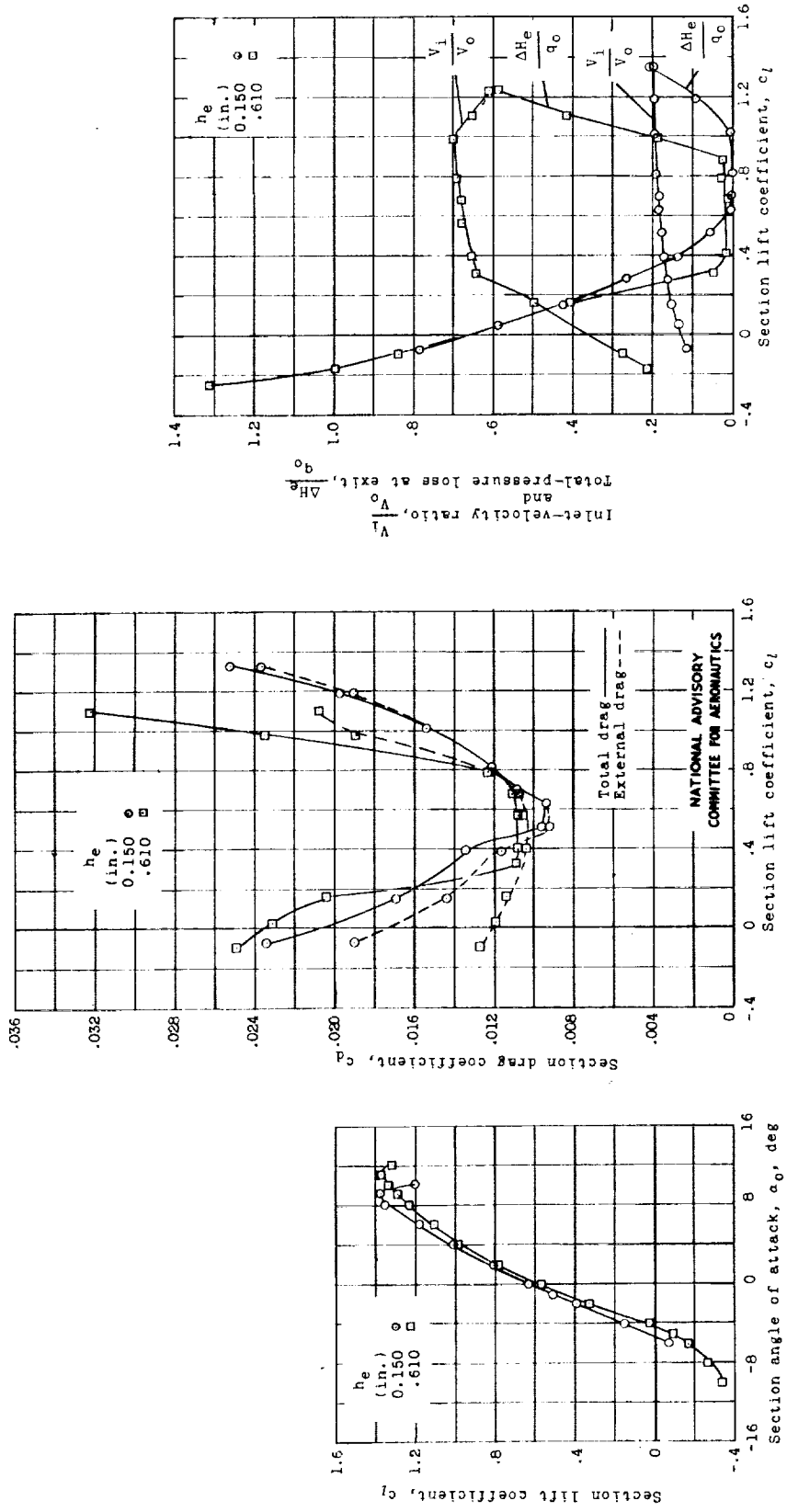

(a) Lift, drag, and flow characteristics.

Figure 6.- Aerodynamic characteristics of the wing-inlet section with inlet 2 and original exit; R, 2.4 X 10^6; test, LTT 369.

L-727

L-727

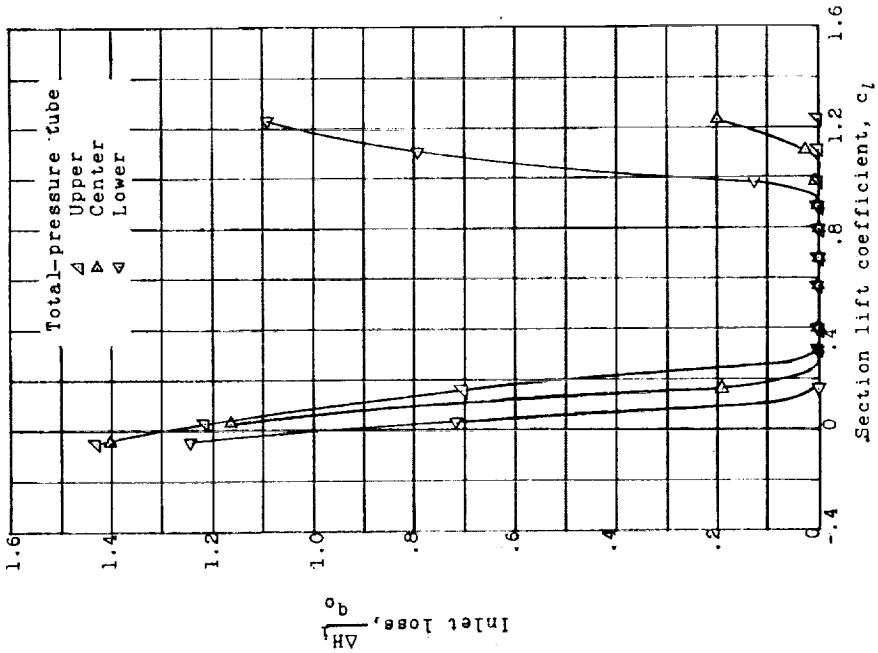

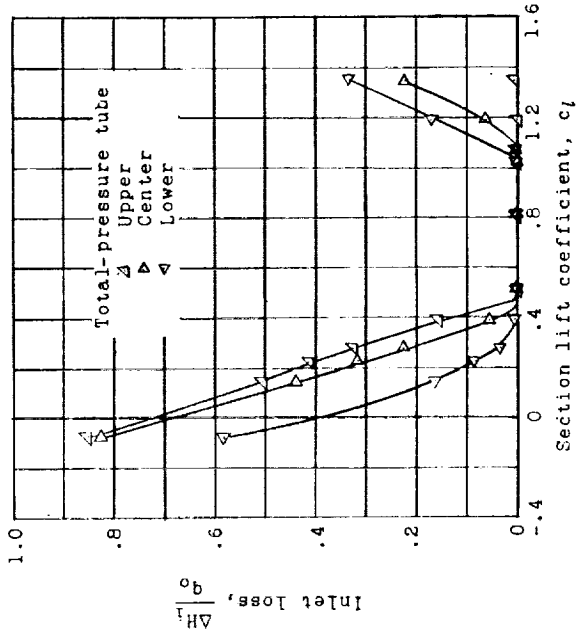

(b) Inlet losses.

Figure 6 .- Concluded.

NATIONAL ADVISORY COMMITTEE FOR AERONAUTICS

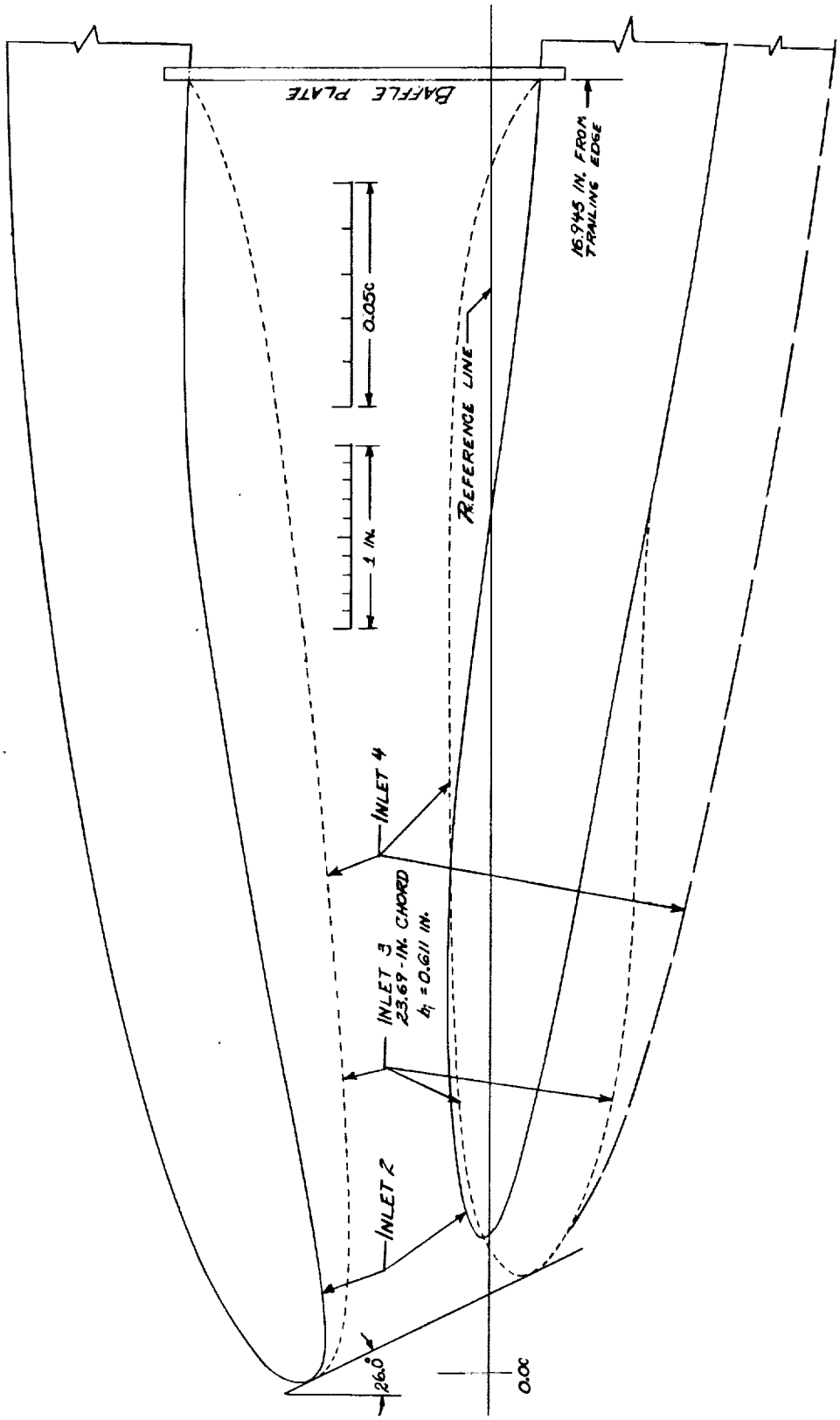

(a) Profiles of inlets 2, 3, and 4.

Figure 7.- Modifications made to form inlets 3 and 4.

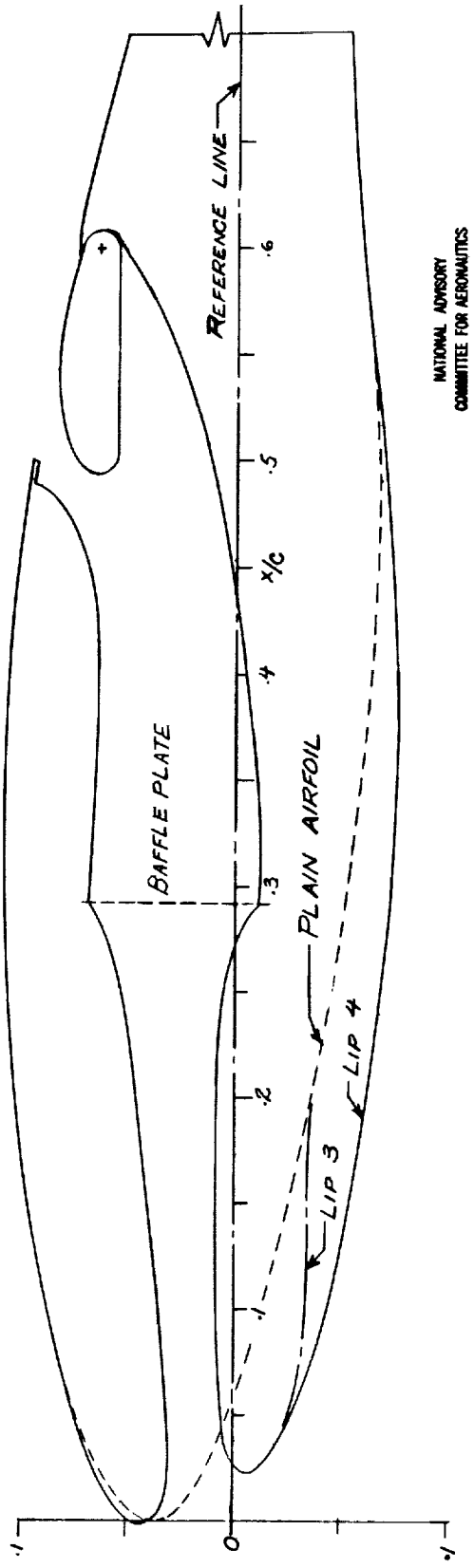

(b) Sketch showing blister required to fair lip 4 into plain airfoil section.

Figure 7.- Concluded.

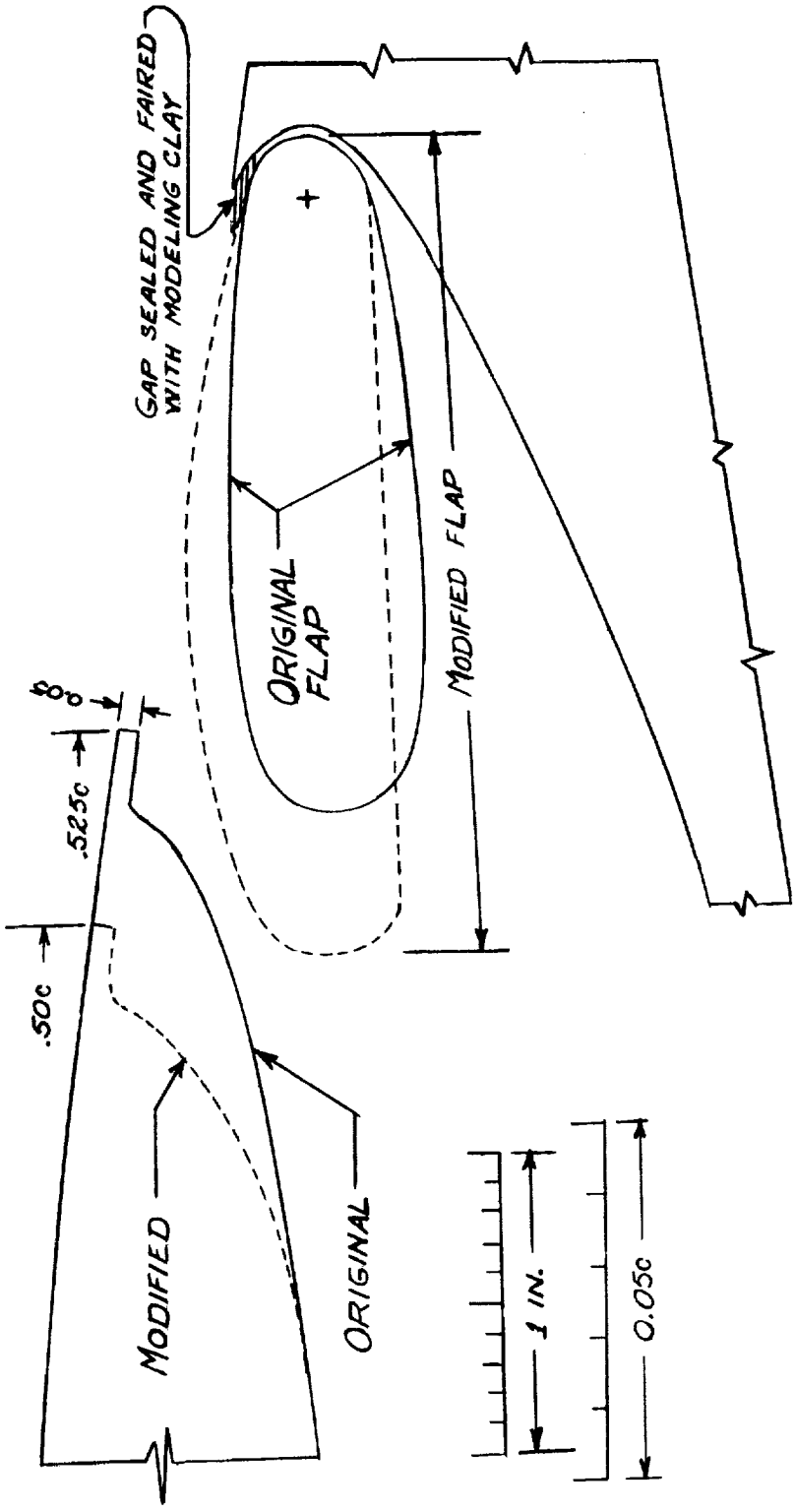

Figure 8.- Sketch of exit modifications.

L-727

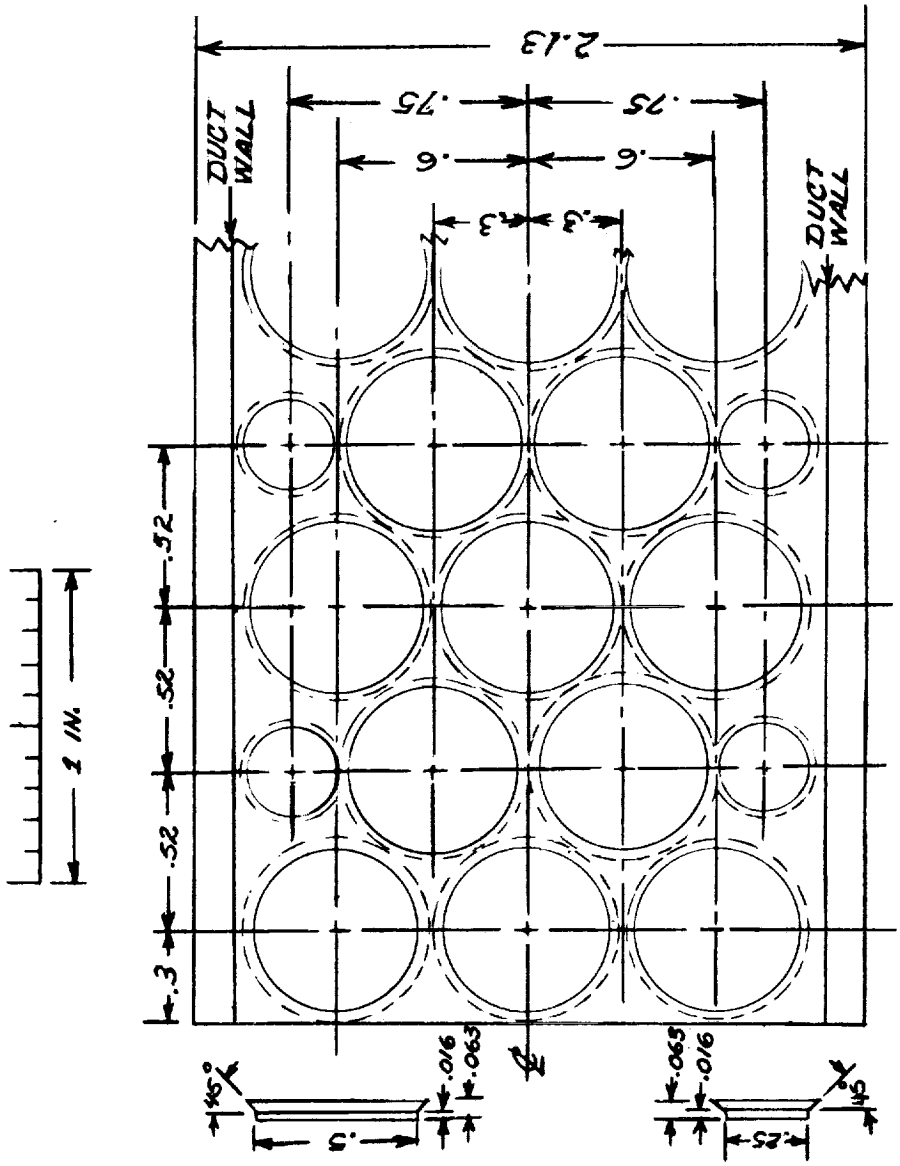

NATIONAL ADVISORY COMMITTEE FOR AERONAUTICS

Figure 9.- Sketch of baffle plate.

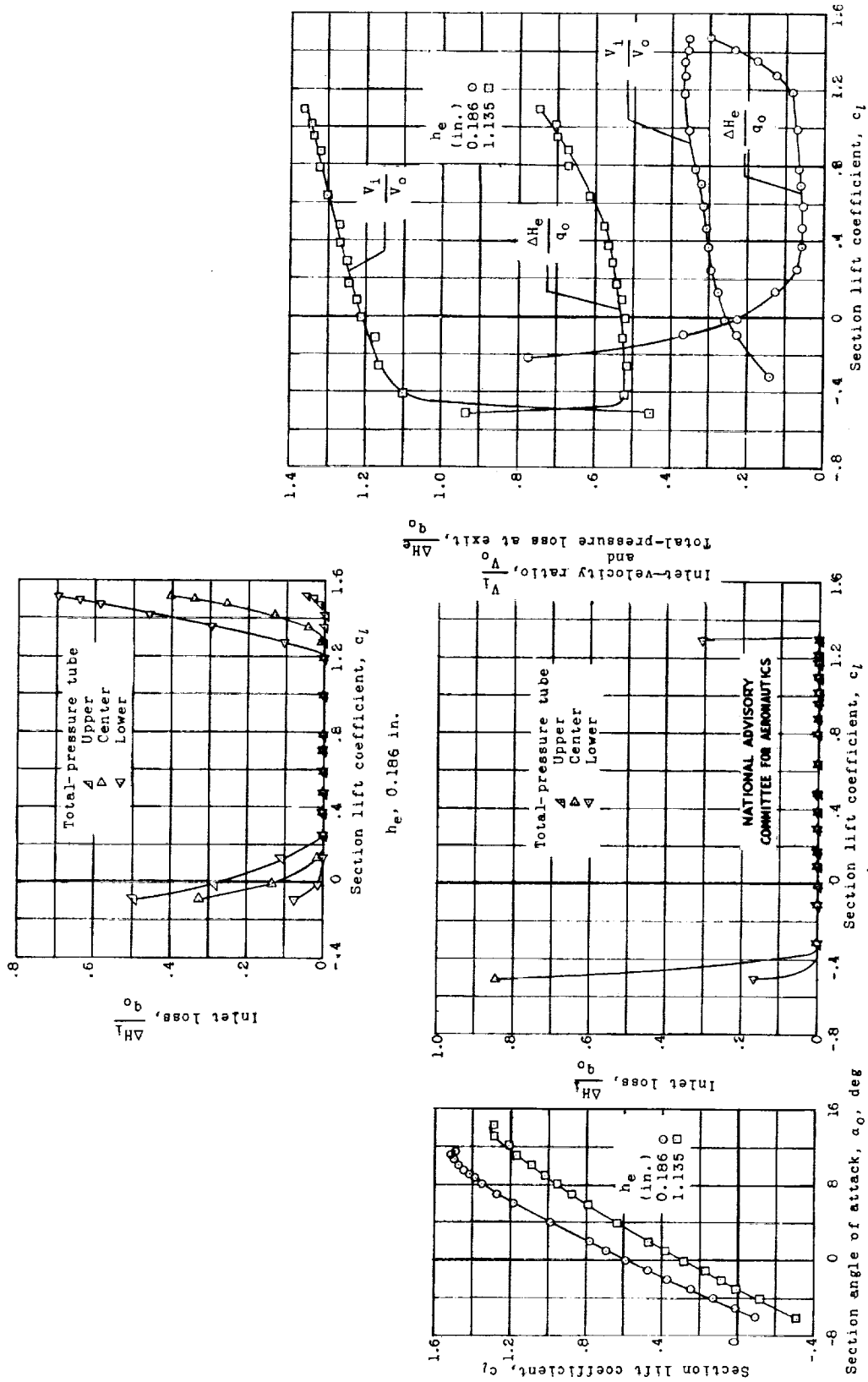

(a) Lift and flow characteristics.

Figure 10.- Aerodynamic characteristics of the wing-inlet section with inlet 3, modified exit, and baffle plate in duct; R, 2.4 X 10⁶; test, LTT 380.

L-727

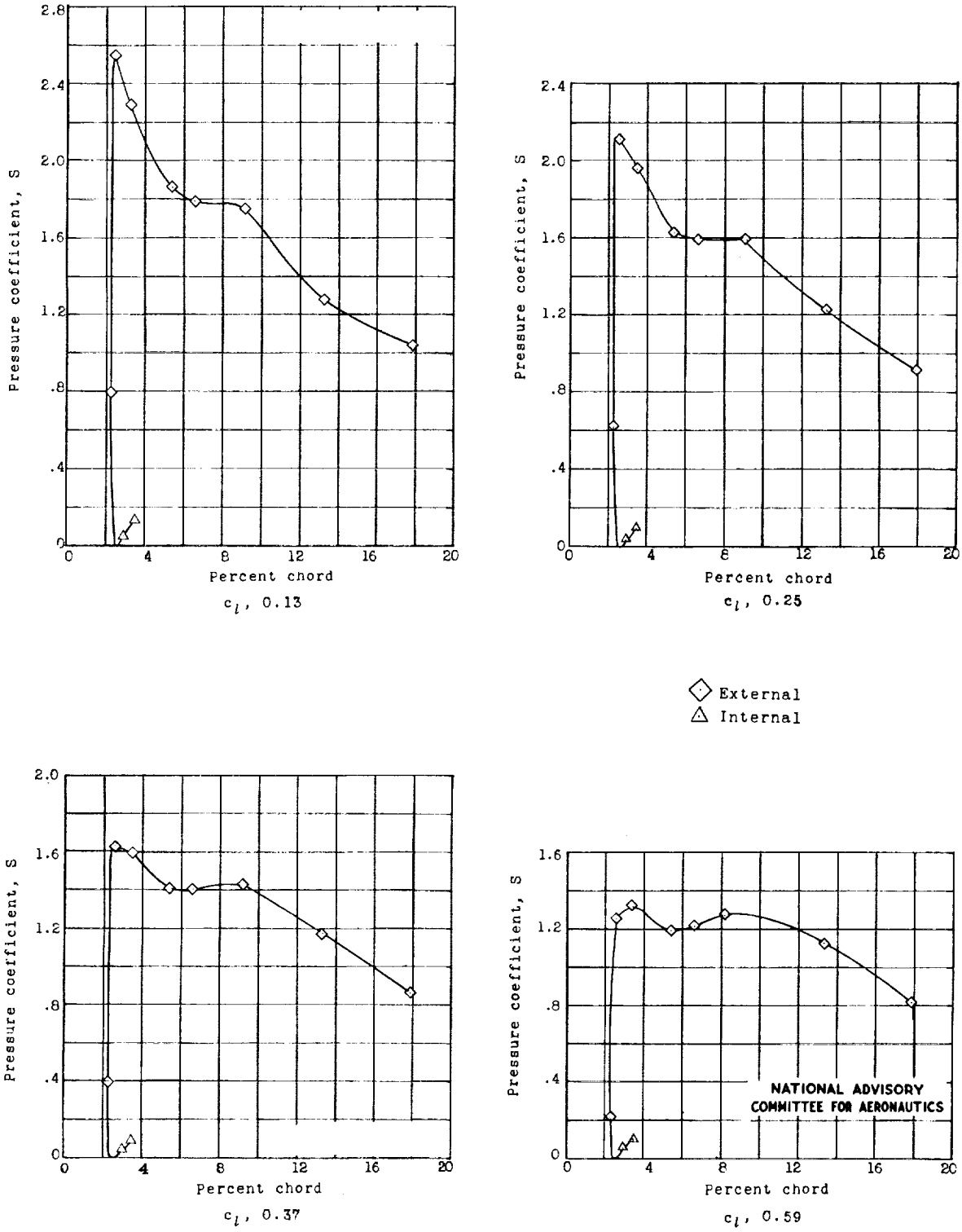

(b) Pressure distributions, lower surface; h_e, 0.186 inches.

Figure 10.- Concluded.

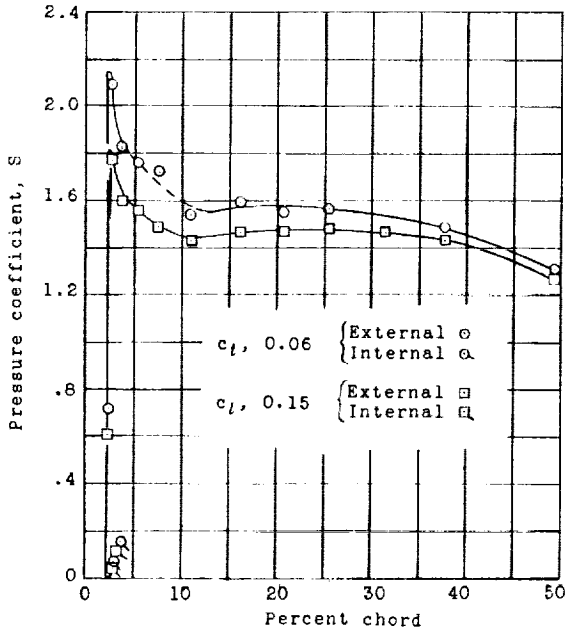

c_l, 0.06 and 0.15

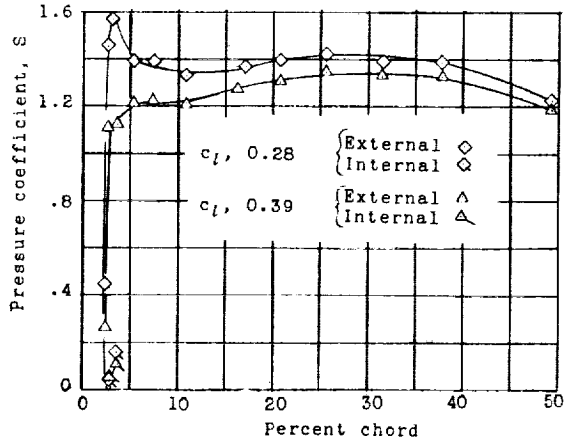

c_l, 0.28 and 0.39

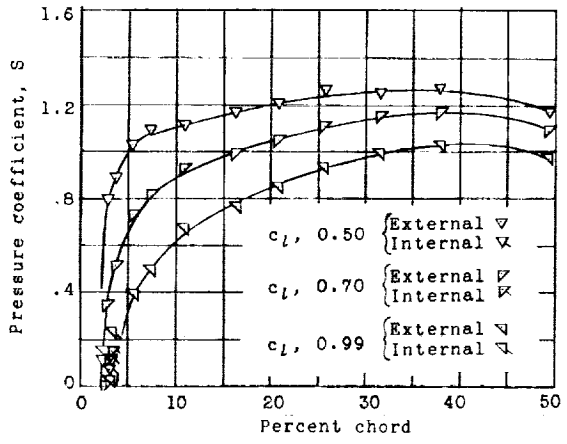

c_l, 0.50, 0.70, and 0.99

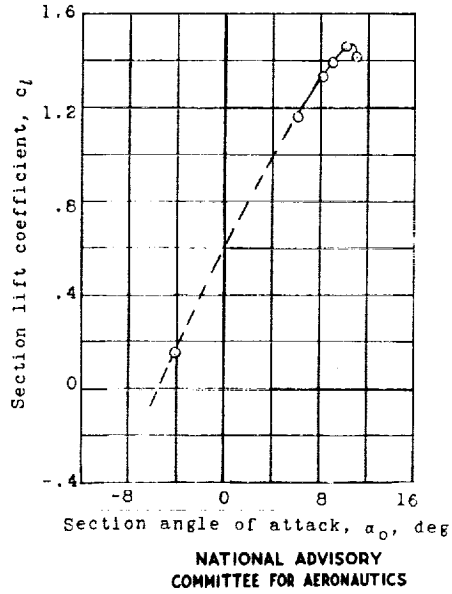

Figure 11.- Pressure distributions on the lower surface and lift characteristics of the wing inlet section with inlet 4, modified exit, and baffle plate in duct; h_e, 0.188 inches; R, 2.0 X 10^6; test, LTT 380.

L-727

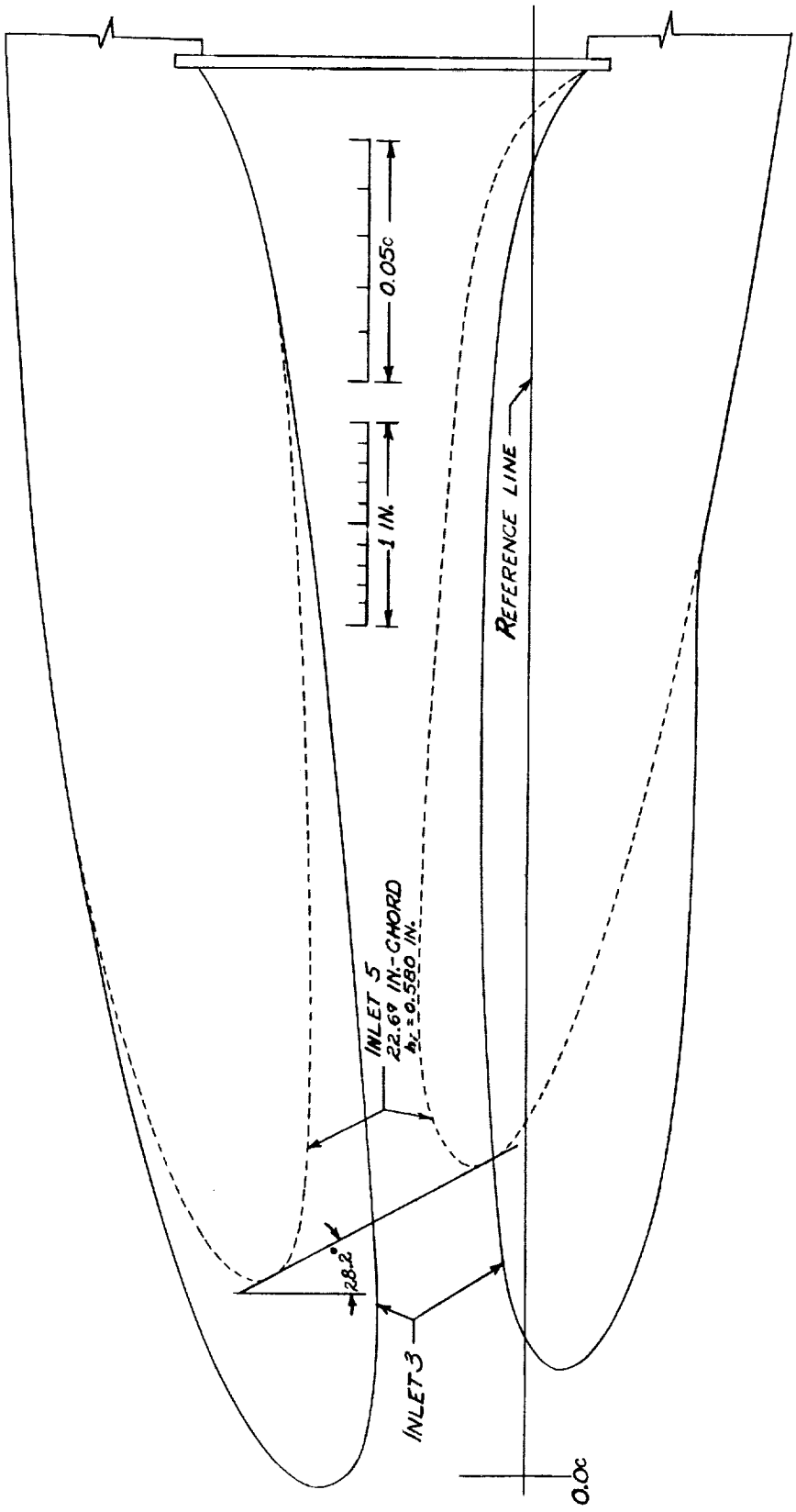

NATIONAL ADVISORY COMMITTEE FOR AERONAUTICS

Figure 12.- Profiles of inlets 3 and 5.

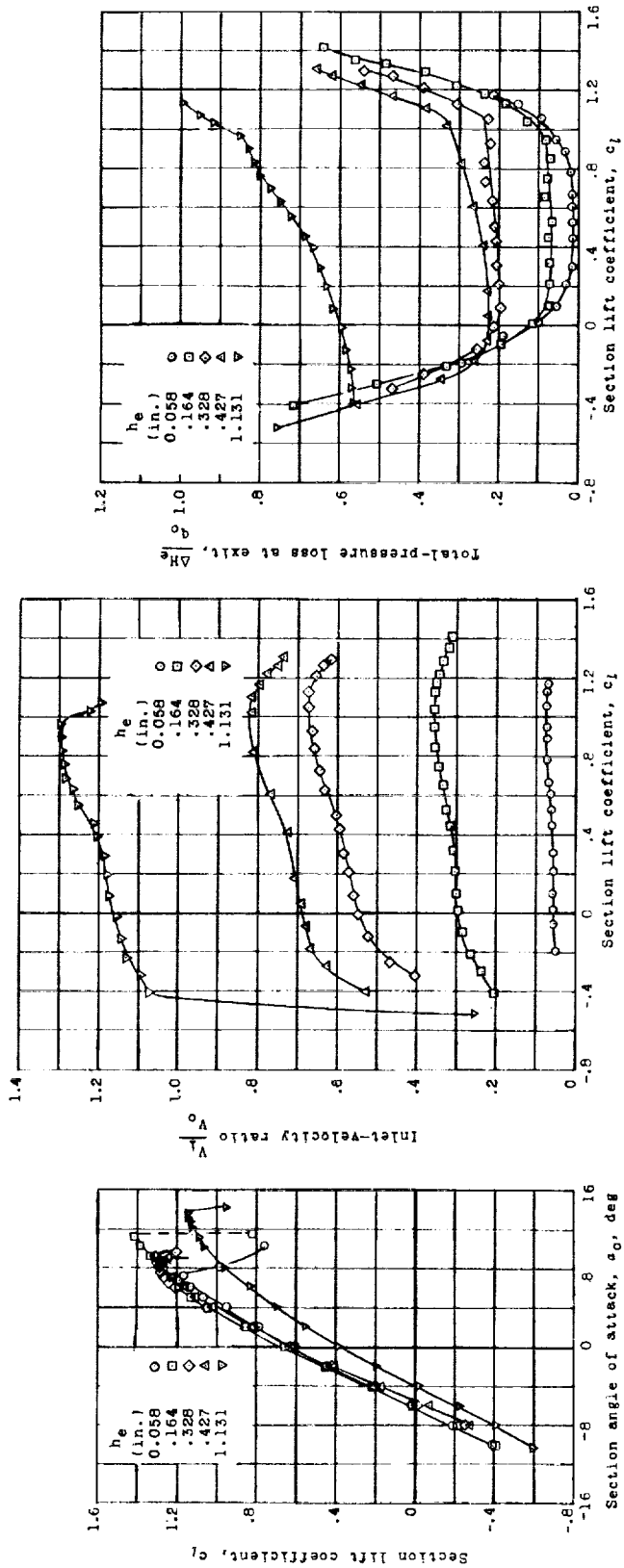

(a) Lift and flow characteristics: R, 2.3 X 10^6.

Figure 13.- Aerodynamic characteristics of the wing inlet section with inlet 5, modified exit, and baffle plate in duct: tests, LTT 399 and TDT 763.

L-727

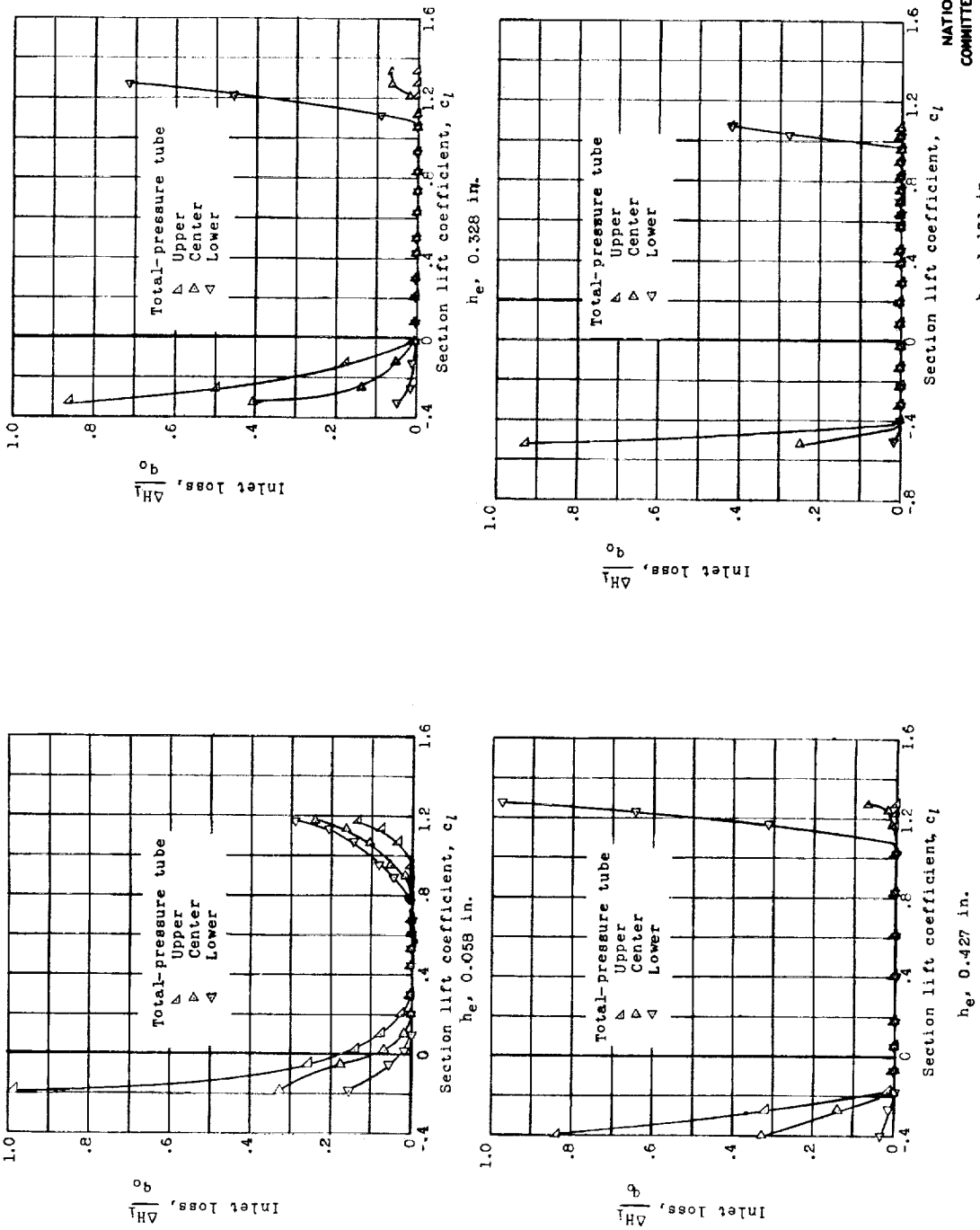

(b) Inlet losses: R, 2.3×10^6.

Figure 13.- Continued.

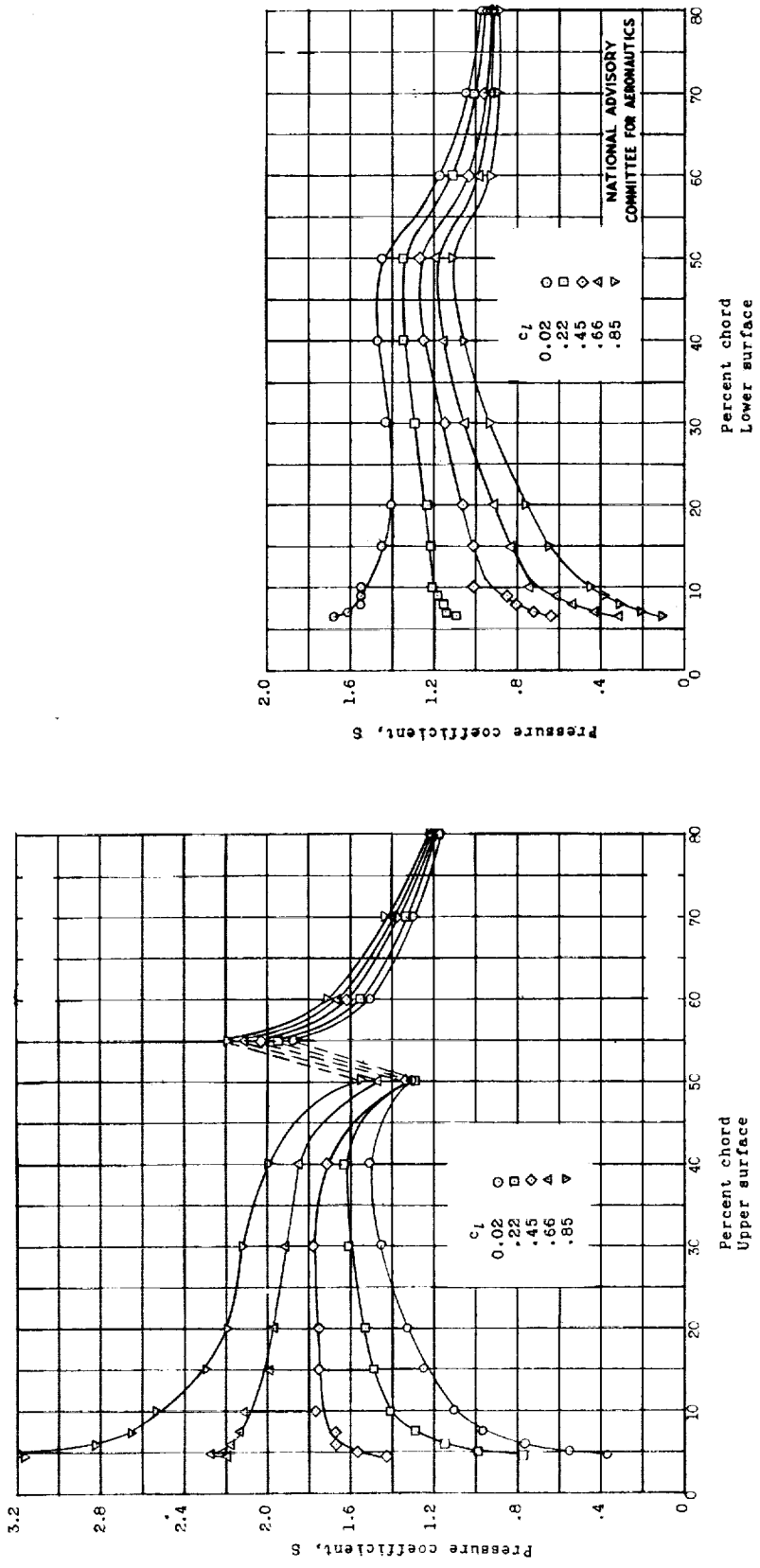

(c) Pressure distributions; h_e, 0.164 inches; R, 2.3 X 10^6.

Figure 13.- Continued.

L-727

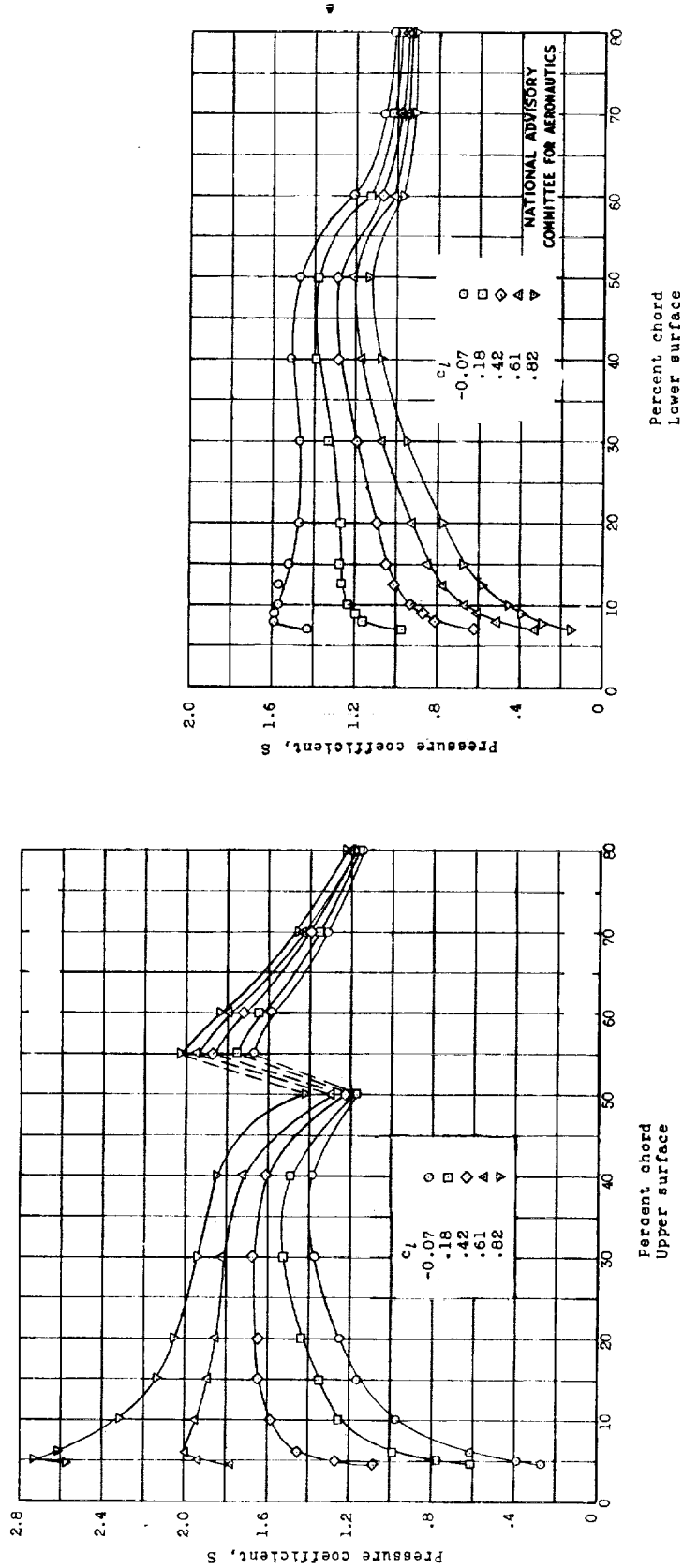

(d) Pressure distributions: h_e, 0.427 inches; R, 2.3 X 10^6.

Figure 13.- Continued.

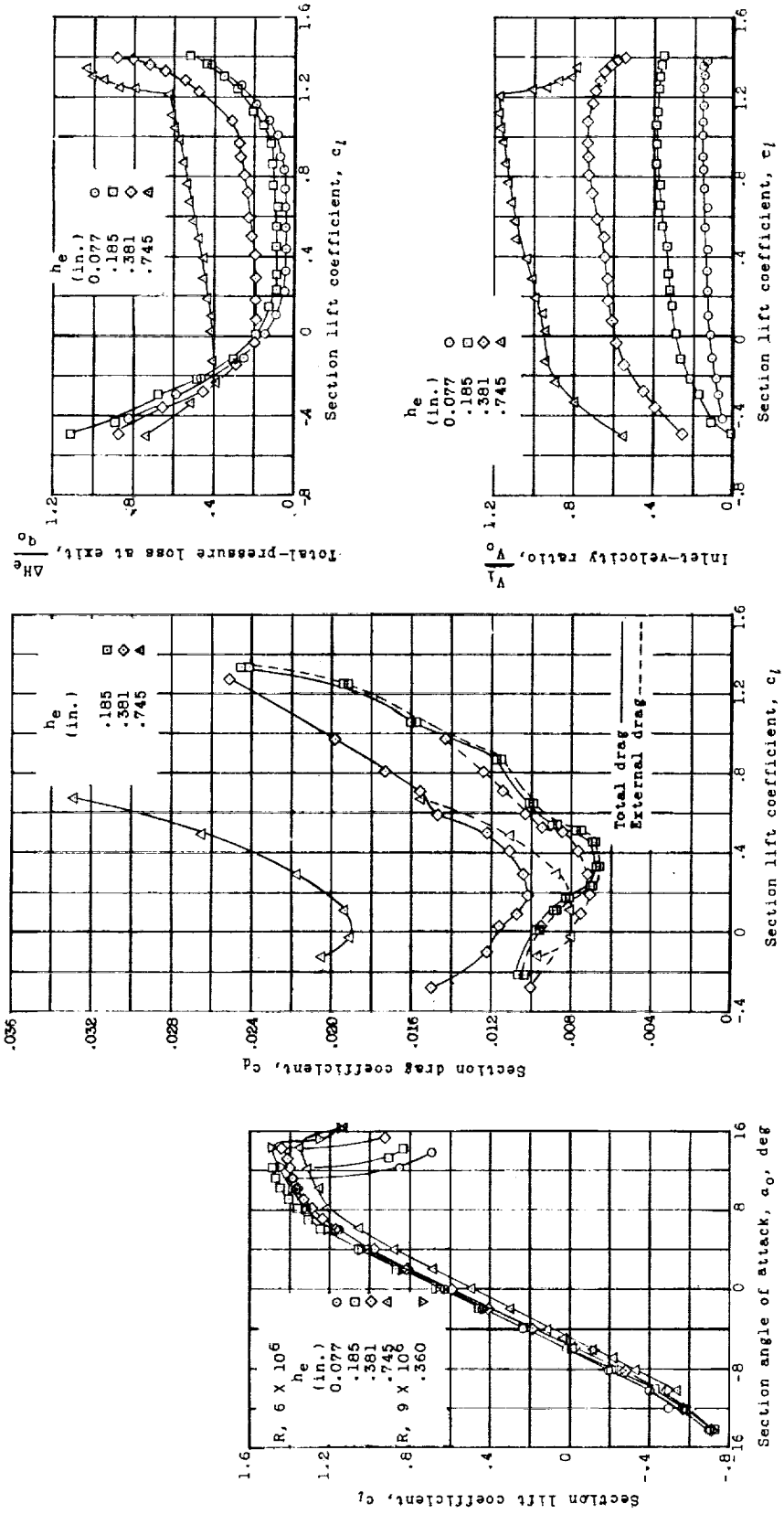

NATIONAL ADVISORY COMMITTEE FOR AERONAUTICS

(e) Lift, drag, and flow characteristics; R, 6 X 10^6.

Figure 13.- Continued.

L-727

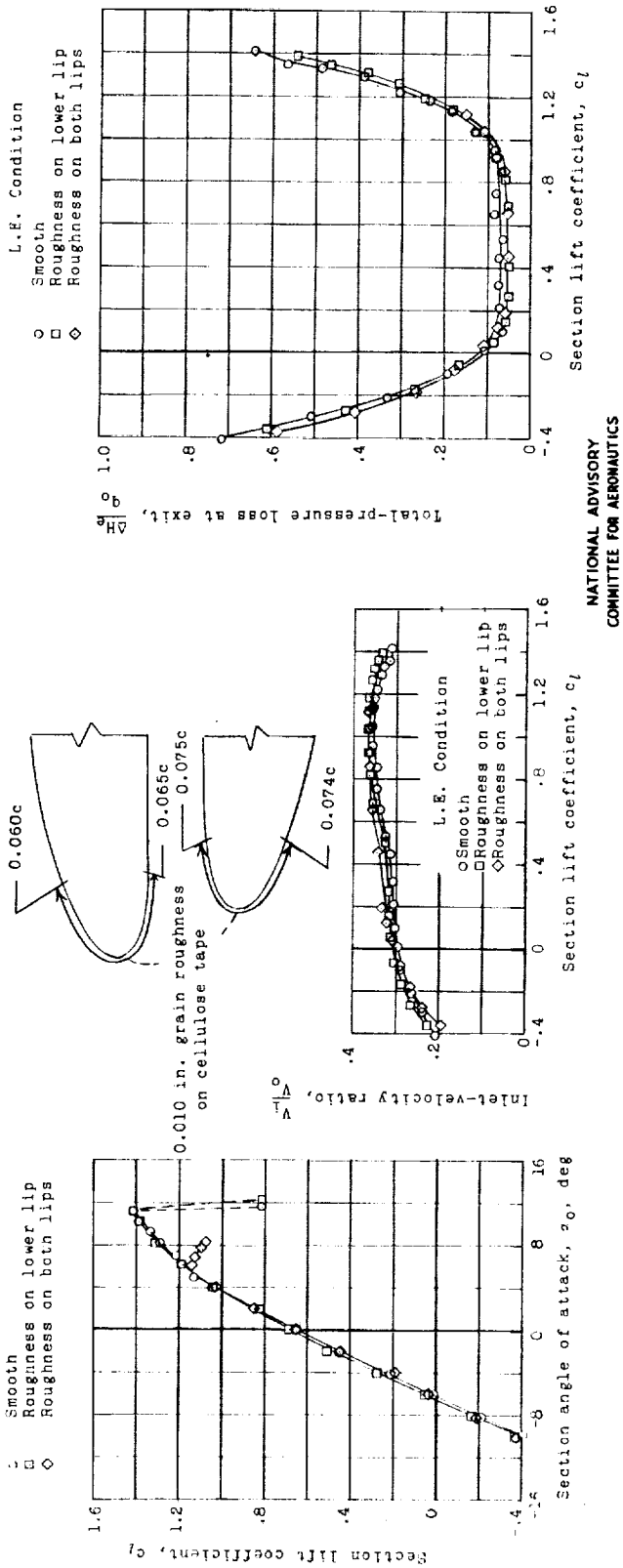

(f) Lift and flow characteristics with and without leading-edge roughness: n_e, 0.164 inches; R, 2.3 X 10^6.

Figure 13.- Concluded.

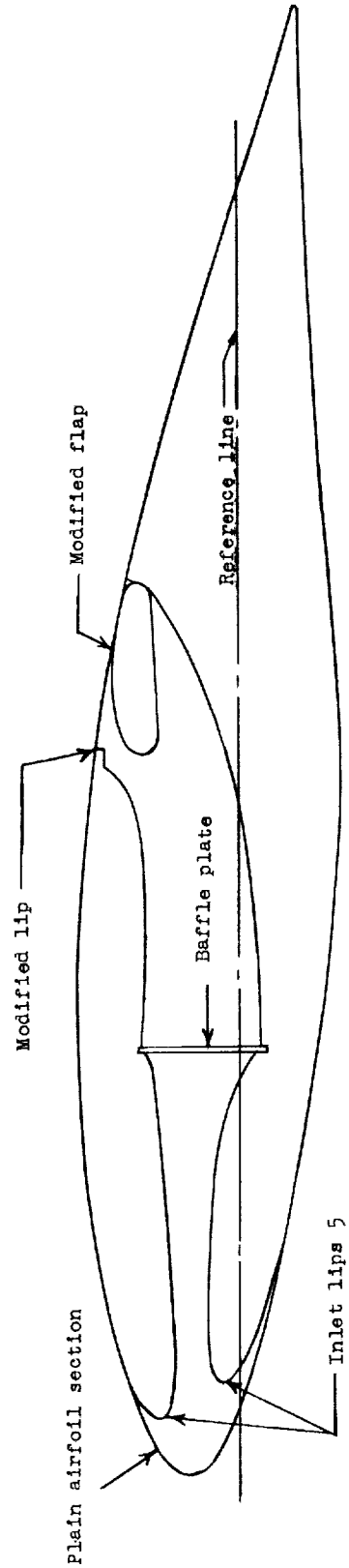

NATIONAL ADVISORY
COMMITTEE FOR AERONAUTICS

(a) Profiles of inlet 5 and plain airfoil section.

Figure 14.- Details of the half-span ducted airfoil section.

L-727

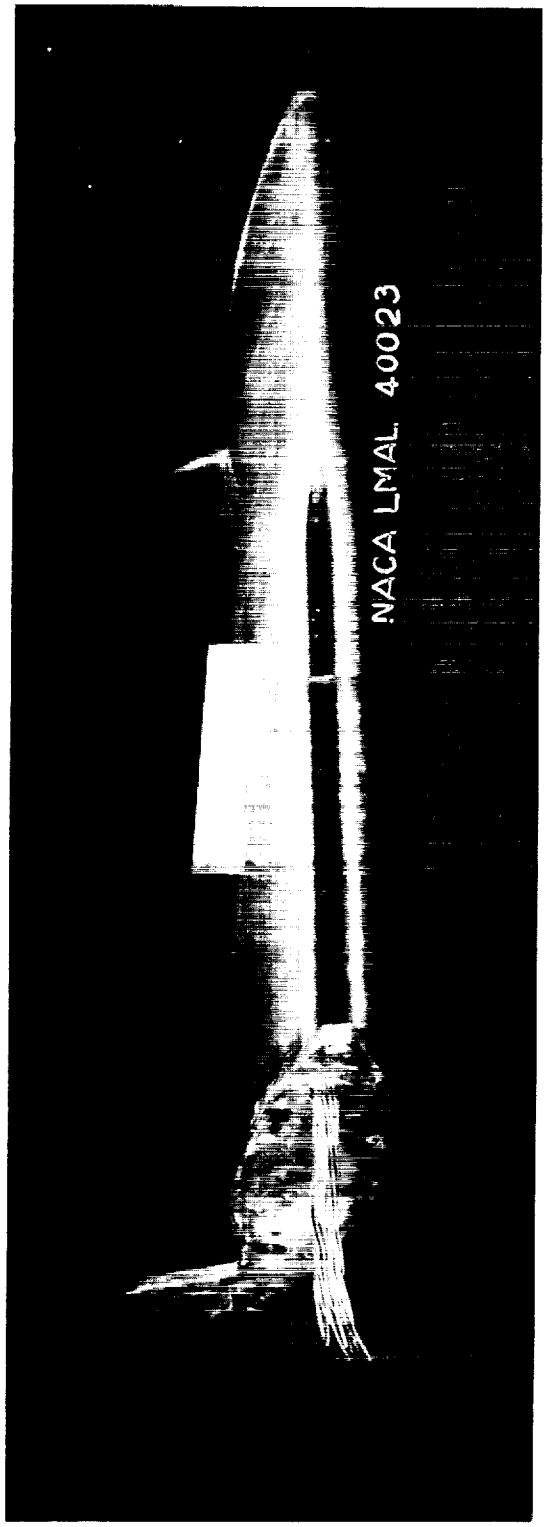

(b) Three-quarter view of model inverted showing fairing between ducted and plain airfoil sections.

Figure 14.- Continued.

L-727

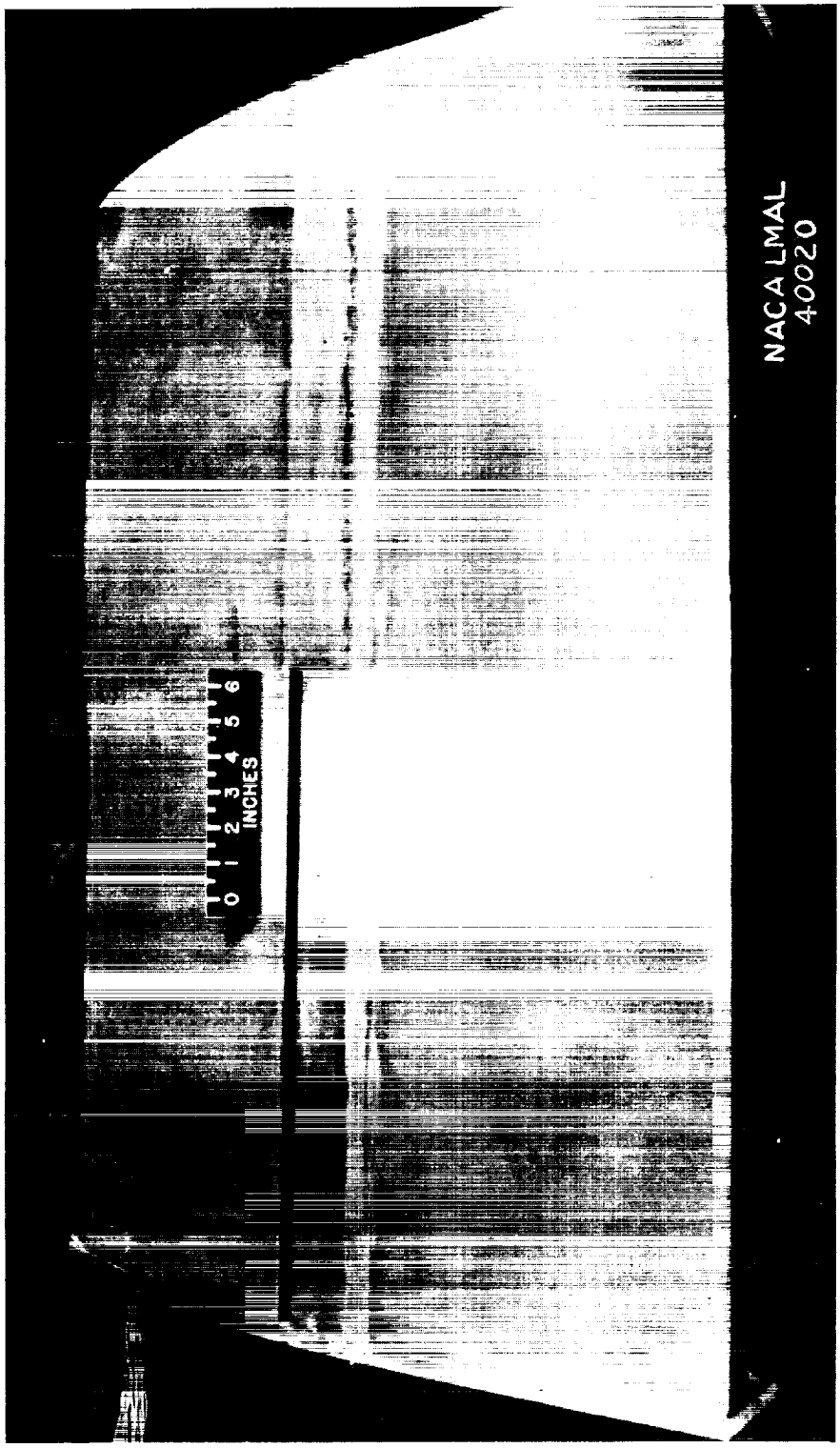

(c) Top view showing exit of ducted section.

Figure 14.- Concluded.

L-727

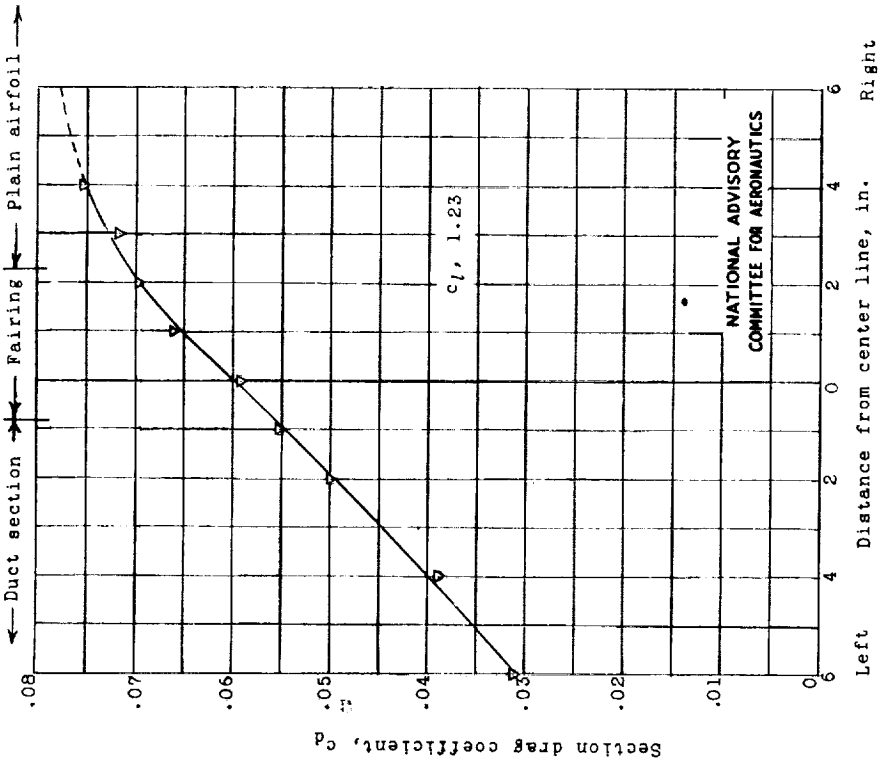

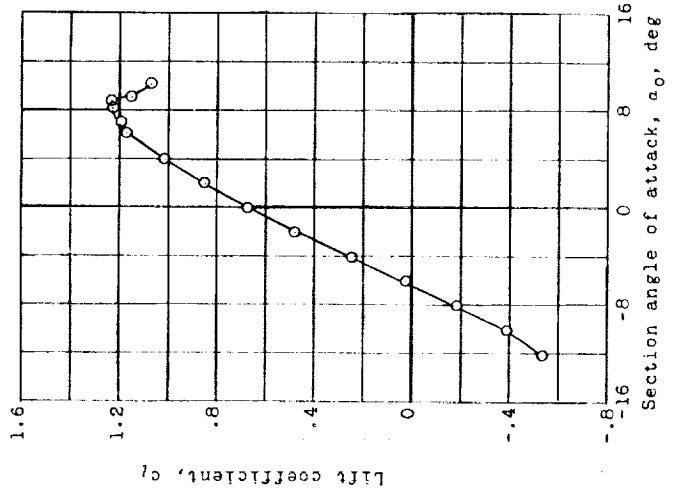

Figure 15.- Aerodynamic characteristics of the transition section with inlet 5, modified exit, and baffle plate in duct: h_e, 0.360 inches; R, 2.4×10^6; test, LTT 388.

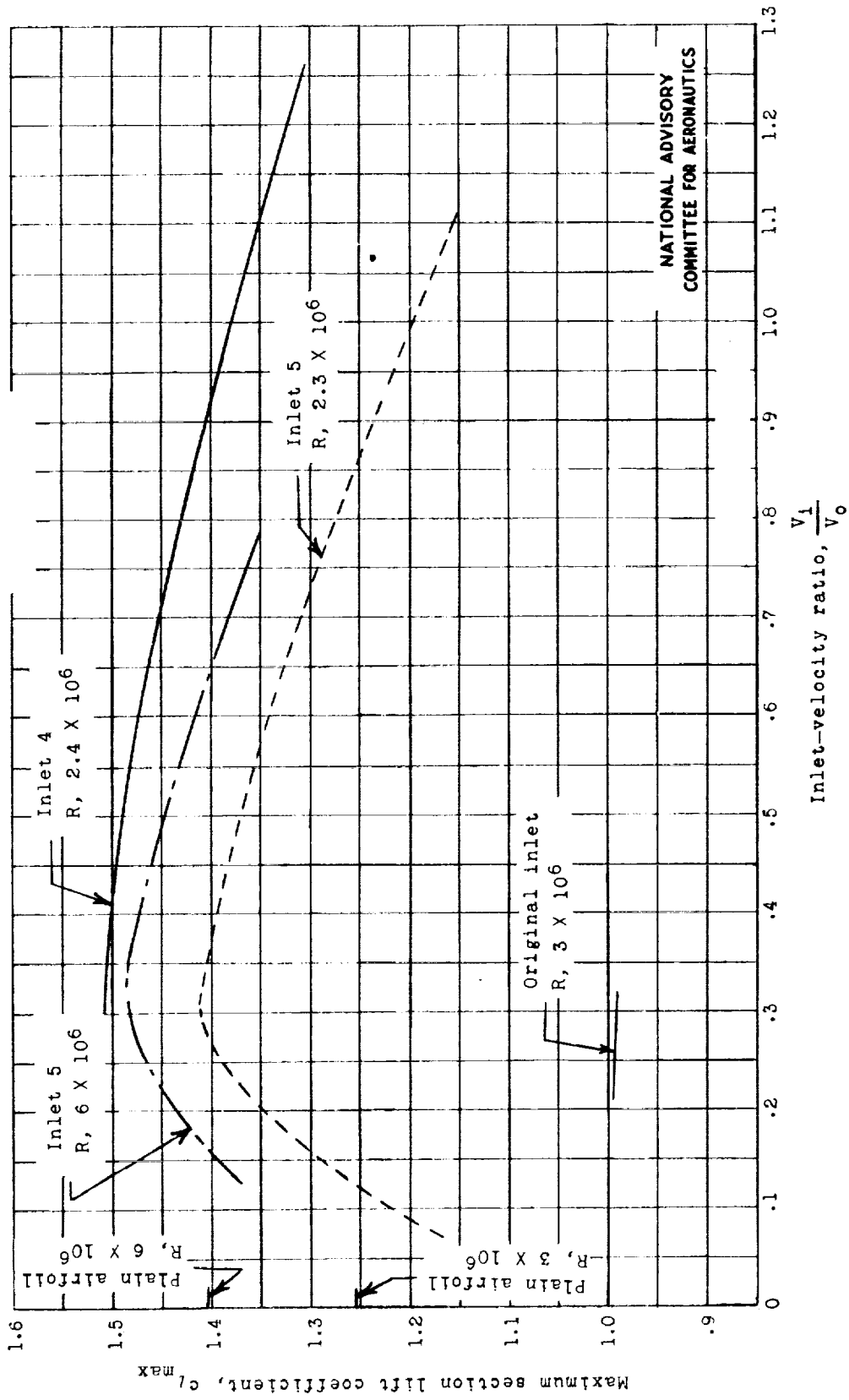

(a) Maximum lift characteristics.

Figure 16.- Comparison of the characteristics of the wing-inlet section.

E-727

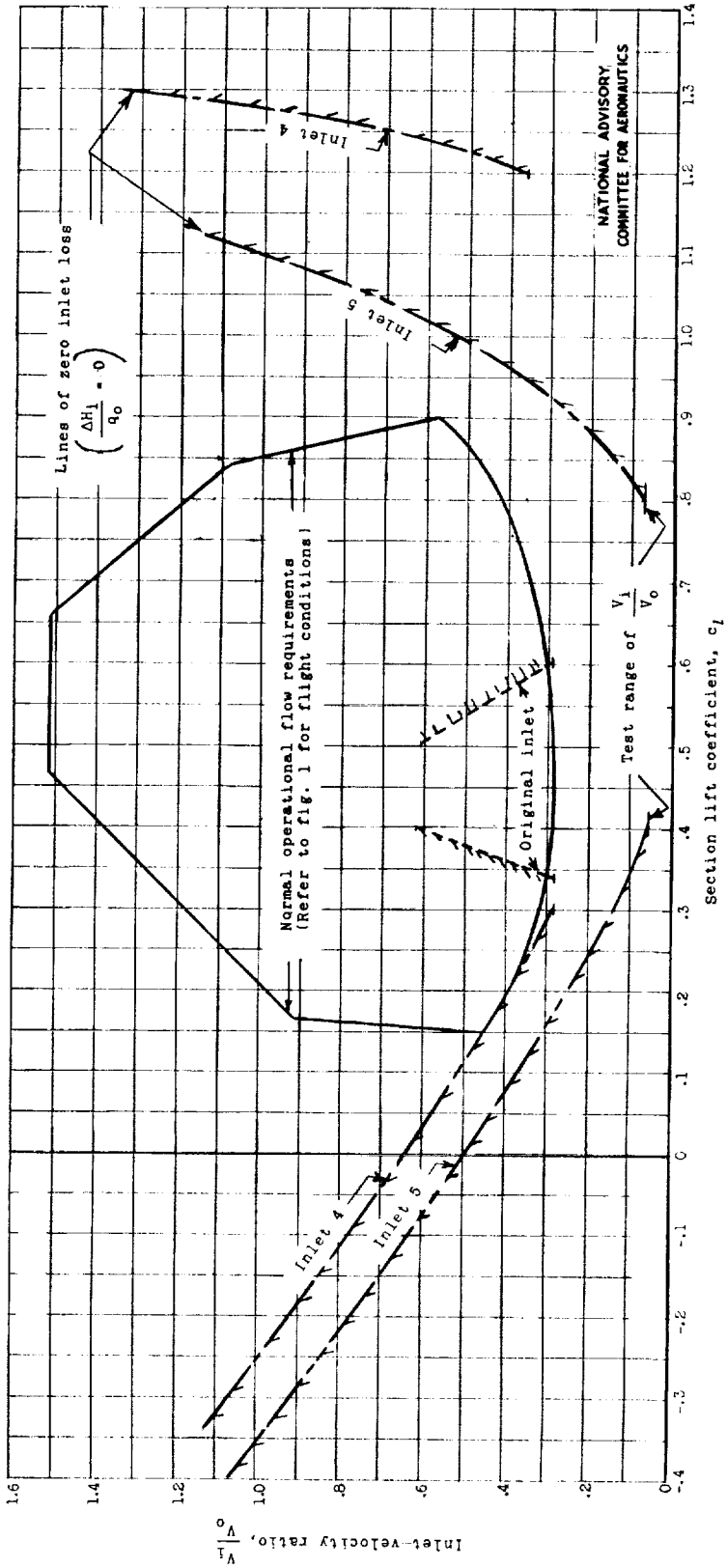

(b) Operating limits for zero inlet loss.

Figure 16.- Continued.

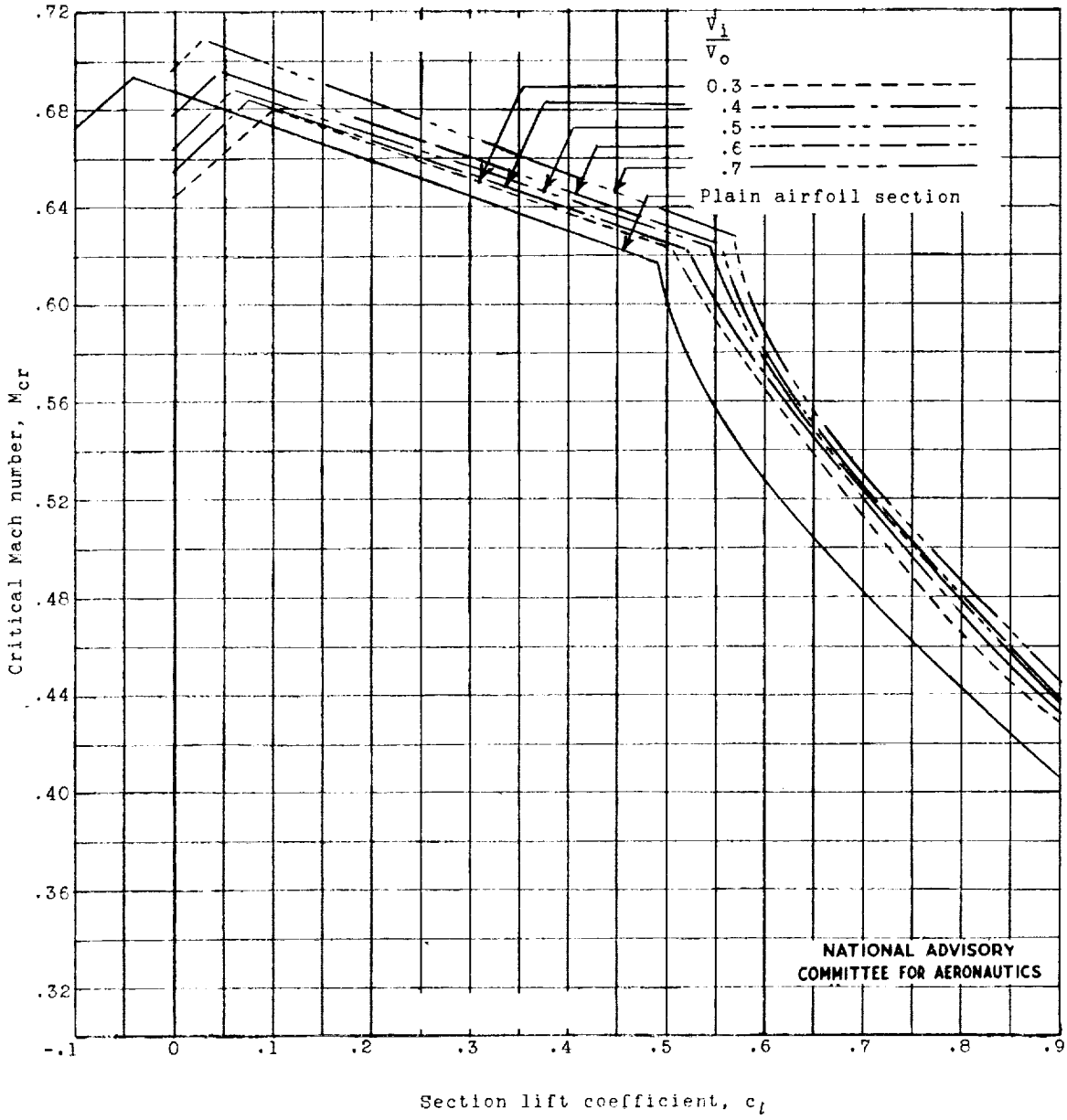

(c) Comparison of predicted critical Mach number of inlet 5 and plain airfoil section.

Figure 16.- Continued.

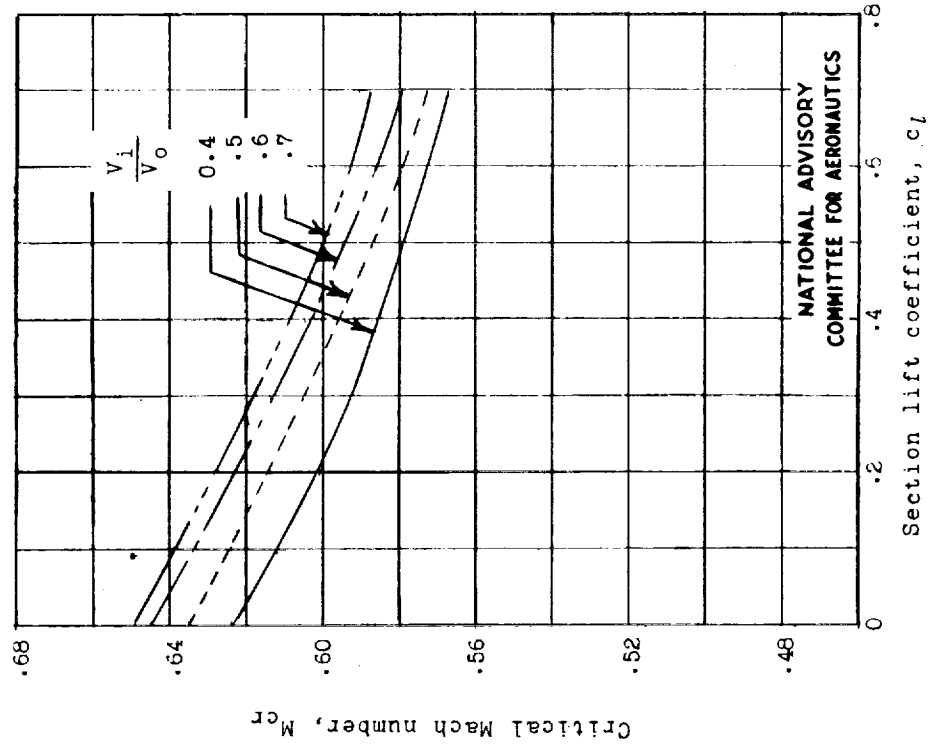

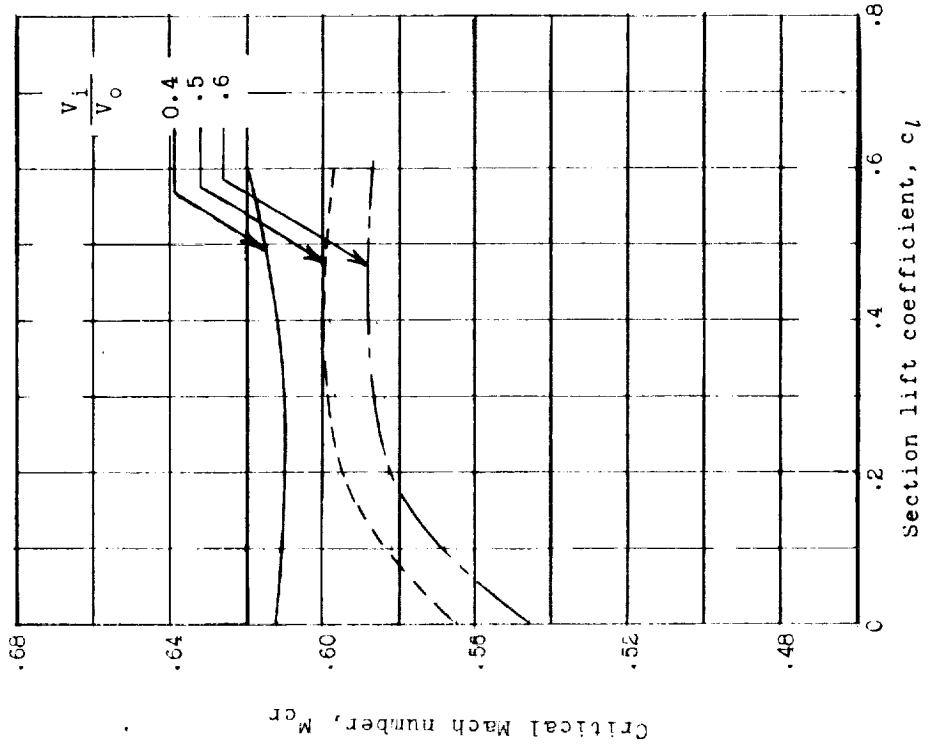

(d) Predicted critical Mach number corresponding to pressure measured at exit.

Figure 16.- Concluded.